



Hadley Centre technical note 74

*W.J. Collins, N. Bellouin, M. Doutriaux-Boucher, N. Gedney,
T. Hinton, C.D. Jones, S. Liddicoat, G. Martin, F. O'Connor,
J. Rae, C. Senior, I. Totterdell, S. Woodward.
T. Reichler and J. Kim.*27

27 November 2008



Evaluation of the HadGEM2 model

W.J. Collins, N. Bellouin, M. Doutriaux-Boucher, N. Gedney, T. Hinton, C.D. Jones, S. Liddicoat, G. Martin, F. O'Connor, J. Rae, C. Senior, I. Totterdell, S. Woodward.
Met Office Hadley Centre, Exeter, UK

T. Reichler and J. Kim.

Department of Meteorology, University of Utah, Salt Lake City, Utah

Executive Summary

- The climate in HadGEM2 is significantly improved over HadGEM1
- The physical climate is now able to sustain a realistic vegetation distribution
- Issues with the Indian monsoon and ENSO will be addressed in HadGEM3
- The earth system components have been evaluated as fully meeting the requirements for an Earth System GCM.

The HadGEM2 model is a two stage development from HadGEM1, representing improvements in the physical model and the addition of earth system components and coupling.

The HadGEM2 project targeted two key features of physical performance: ENSO and northern continent land-surface temperature biases. The latter had a particularly high priority in order for the model to be able to adequately model continental vegetation. Through focussed working groups we identified a number of mechanisms that improved the performance. Some known systematic errors in HadGEM1, such as the Indian monsoon, were not targeted for attention in HadGEM2.

HadGEM2 has substantially improved mean SSTs and wind stress and improved tropical SST variability compared to HadGEM1. The northern continental warm bias in HadGEM1 has been significantly reduced. The power spectrum of El Nino is made worse, but other aspects of ENSO are improved. Overall there is a noticeable improvement from HadGEM1 to HadGEM2 when comparing global climate indices, putting HadGEM2 in a leading position compared to the CMIP-3 models.

The earth system components are shown to perform well. The TRIFFID vegetation scheme had been used in a configuration from a previous generation of Hadley Centre models (HadCM3LC). In HadGEM2 the vegetation cover is better than in the HadCM3LC model especially for trees. The presence of too much bare soil in Australia though causes problems for the dust emissions scheme. The simulation of global soil and biomass carbon stores are good and agree well with observed estimates except in regions of errors in the vegetation cover. HadGEM2 compares well with the C4MIP ensemble of models. The distribution of NPP is much improved relative to HadCM3LC. At a site level the component carbon fluxes validate better

against observations and in particular the timing of the growth season is significantly improved. The seasonal cycle of atmospheric CO₂ concentrations compare extremely well to observations.

The ocean biology (diat-HadOCC) allows the completion of the carbon cycle and the provision of di-methyl sulphide (DMS) emissions from phytoplankton. DMS is a significant source of sulphate aerosol over the oceans. The diat-HadOCC scheme is an improvement over the standard HadOCC scheme as it differentiates between diatom and non-diatom plankton. These have different processes for removing carbon from the surface to the deep ocean, and respond differently to iron nutrients. The HadOCC scheme performs well with very reasonable plankton distributions, rates of productivity and emissions of DMS.

The additions of a tropospheric chemistry scheme, new aerosol species (organic carbon and dust) and coupling between the chemistry and sulphate aerosols have significantly enhanced the earth system capabilities of the model. This has improved the tropospheric ozone distribution and the distributions of aerosol species compared to observations, both of which are important for climate forcing.

Including interactive earth system components has not significantly affected the physical performance of the model. The components themselves compare well with observations and other models. Therefore we can conclude that HadGEM2 fully meets the requirements of an Earth System GCM. It will be a valuable tool for the Hadley Centre to predict future climate and understand the climate feedbacks within the earth system.

1. Introduction

HadGEM2 is the product of two development projects: improving the physical climate; and adding earth system components and couplings. It is the first Met Office Hadley Centre earth system model to run without the need for flux corrections. A previous carbon cycle model in the Hadley Centre (HadCM3LC) (Cox et al. 2001) had to use artificial correction terms to keep the model state from drifting uncontrollably. Most other carbon cycle models in the community need these corrections. For the purposes of this note, where clarification is necessary, the configurations without earth system components will be denoted HadGEM2-A and HadGEM2-AO (atmosphere and atmosphere-ocean respectively). The model with the earth system components will be denoted by HadGEM2-ES.

1.1. Progress between HadGEM1 and HadGEM2-AO.

The aim of the physical component of the HadGEM2 project has been to improve two key features of the performance of HadGEM1: the simulation of ENSO and a reduction of land-surface temperature biases over northern continents. HadGEM1 is described in Johns et al. (2006). Tropical SST variability in HadGEM1 is somewhat weak, but the bigger problem is the lack of a 'SO' response in the atmosphere. Land surface biases in HadGEM1 are so large that when coupled to an earth-system model, the vegetation over these regions is very unrealistic and hence bio-geophysical feedbacks are not adequately represented.

Here we highlight the improvements made in HadGEM2 in these features. Key mechanisms have been identified and physical changes have been implemented that

have led to substantial improvements in the two key features. In the atmosphere, we have implemented an adaptive detrainment parameterization in the convection scheme which has improved the simulation of tropical convection and led to a much reduced (and more realistic) wind stress over the tropical Pacific. We have changed the treatment of excess water from super-saturated soil surfaces, included a background climatology of biogenic aerosols, and improved the representation of the lifetime of convective cloud - all of which have led to reductions in the land surface warm bias over northern continents. In the ocean, we have identified a 10-year timescale drift in global SSTs related to adjustments in the upper ocean. This has led us to change the background ocean diffusivity profile in the thermocline, which has substantially reduced SST drift in the tropics and given a reasonably balanced Top-Of-the-Atmosphere (TOA) radiative flux ($\sim 0.5 \text{ W m}^{-2}$)¹. These improvements in the mean state (SST, wind stress) in the tropical Pacific are in turn related to apparent improvements in El-Nino variability and the 'SO' response in the atmosphere. Table 1.1 lists the main differences between HadGEM2-AO against the HadGEM1 control. Whilst the focus was on improving ENSO and land surface temperatures, a number of other changes were included, (a) to correct bugs, and (b) to improve physical characteristics where such improvements were available and relevant for a model to be used for studying Earth system feedbacks (e.g. aerosols). HadGEM2 has the same horizontal and vertical resolution as HadGEM1 in both the atmosphere and ocean. A detailed analysis of the use of a broad range of timescales to identify systematic errors and develop solutions for the physical processes in HadGEM2 will be reported in a further paper (Martin et al. in preparation).

1.2. Vertical configurations of the model

The evaluation presented here covers two configurations of the atmospheric model; 38 levels (L38) extending to 40km (upper stratosphere), and 60 levels (L60) extending to 85km (mesopause). Inclusion of the mesosphere is essential to simulate properly the wave-driving responsible for the stratospheric circulation. As well as an increased height of the model top, the L60 configuration has more than a factor of two better vertical resolution within the stratosphere. The improved representation of the stratosphere may prove important in identifying climate couplings, such as those driving variability in the North Atlantic Oscillation (NAO).

The carbon cycle is relatively independent of the influence of the stratosphere; hence the standard configuration HadGEM2 Earth System Model will be at L38. The L60 model will be used to identify future changes in modes of climate variability. The L60 model has also been delivered to the UKCA project for research on stratospheric ozone.

¹ Since the top-of-atmosphere flux was tuned, a bug has been found in the Rayleigh scattering code. Fixing this bug has introduced a substantial ($\sim 1 \text{ W m}^{-2}$) decrease in the TOA flux. The model is currently being re-tuned to offset this imbalance.

	Differences between HadGEM2-AO and HadGEM1	Reason for change	References
Aerosols	Sulphate mass now lies in optically-efficient accumulation mode; biomass burning aerosols experience hygroscopic growth	Representation of aerosols is more now realistic, based on observations gathered from dedicated field campaigns.	<i>Bellouin et al., 2007;</i> <i>Haywood et al., 2003</i>
	Mineral dust and secondary organic aerosols included	Two important natural aerosol species are now represented in the model	See appendix A for details of the dust scheme
Convection	Inclusion of ‘adaptive detrainment’ parameterisation	Produces smoother mass-flux profiles and more realistic diabatic heating profiles	<i>Maidens and Derbyshire, 2006</i>
	Depth criterion for shallow convection removed	To allow shallower clouds to rain provided their water content is sufficiently high	
Boundary Layer	Non-gradient stress parameterisation	Generates improved (more well-mixed) wind profiles in convective boundary layers	Brown and Grant (1997)
	Assorted bug fixes		
Land surface processes	Excess soil water (e.g. through snowmelt) drained out of the bottom of the soil layer instead of being pushed back out of the top layer	Increases soil moisture in lower soil layers and so helps to reduce water-stress on vegetation following snowmelt in Northern Hemispheric continents	Similar to MOSES I (Cox et al., 1999)
Ocean processes	Laplacian viscosity, K_x , is reduced; formally, $K_x = 750(1 - \cos(\phi))m^2s^{-1}$, where ϕ =latitude. HadGEM1 uses a constant value of $2000m^2s^{-1}$	Leads to a reduction in westward currents on the equator, giving better agreement with observations	
	Diffusivity has been lowered in the upper 1000m of the ocean, placing it at the edge of the uncertainty range	Reduces mixing with cooler subsurface water, increasing the SSTs and also the subsurface cooling in the tropics.	See <i>Moum and Osbourne, 1986</i> for uncertainty range.
River runoff	Enhances vertical and horizontal diffusion in the ocean wherever a river outflow point is present	Corrects a known systematic salty bias close to the Amazon, at a depth of 150m.	
Sea-ice	Bug-fix to the sea-ice albedo parameterisation		

Table 1.1: Summary of main changes from HadGEM1 to HadGEM2-AO

1.3. Importance of and progress in Earth System aspects between HadGEM2-AO and HadGEM2-ES.

Cox et al. (2000) showed that including the carbon cycle in climate models could dramatically change the predicted response of the HadCM3 model to anthropogenic forcing, from 4.0K to 5.5K by the year 2100. This highlighted the importance of Earth System feedbacks in the climate system, and the necessity of including such feedbacks in climate models in order to predict future climate change.

The new components in the HadGEM2-ES model (see table 1.2) are the terrestrial and oceanic ecosystems, and tropospheric chemistry. The ecosystem components TRIFFID and diat-HadOCC are introduced principally to be able to simulate the carbon cycle and its interactions with the climate. Diat-HadOCC also includes the feedback of dust fertilisation on oceanic carbon uptake. The tropospheric chemistry affects the radiative forcing through methane and ozone, and affects the rate at which sulphur dioxide emissions are converted to sulphate aerosol. In HadGEM2-AO the chemistry is provided through climatological distributions that are unaffected by meteorology or climate. In HadGEM2-ES the UKCA scheme (www.ukca.ac.uk) is used to model the chemistry interactively, allowing it to vary with climate.

1.4. Status of HadGEM2 earth system components.

The HadGEM2 model has been built and evaluated with all the earth system components. The individual components have been tuned successfully and have been combined into the fully coupled model. Evaluation of the earth system components is documented in section 3. These components are found to perform very well, compared to observations and other models, and are certainly sufficient to replicate the desired climate feedbacks. The HadGEM2 model is therefore fit for its purpose. The addition of the earth system components has little effect on the top of atmosphere radiation balance.

	Differences between HadGEM2-ES and HadGEM2-AO	Reason for change
	New Components	
Terrestrial Carbon cycle	TRIFFID dynamic vegetation scheme (Cox 2001) added.	To model the exchange of carbon dioxide between the atmosphere and the terrestrial biosphere
Ocean carbon cycle	HadOCC and diat-HadOCC ocean biology schemes added	To model the exchange of carbon dioxide between the atmosphere and the oceanic biosphere
Atmospheric Chemistry	UKCA tropospheric chemistry scheme added	To allow the ozone and methane radiative forcing fields, and the sulphate oxidant fields to vary with meteorology and climate
Aerosols	Fossil-fuel organic carbon aerosol added	This important anthropogenic aerosol species is now represented in the model
	Improved components	
Hydrology	Large-scale hydrology (Clark and Gedney 2008)	This improves the soil moisture and hence vegetation distribution
Aerosols	Extra sulphate oxidation reaction added.	This improves the winter sulphate concentrations
	New couplings	
Chemistry-radiation	The radiative effects of ozone and methane are now taken from the interactive chemistry	This allows the concentrations of these species to vary with climate and to be consistent with varying tropopause heights.
Chemistry-hydrology	The emissions of methane from wetlands are supplied from the hydrology scheme (Gedney et al. 2004) to the chemistry scheme	The emissions and hence concentrations of methane will vary as climate impacts on the extent of wetlands
Chemistry-Aerosols	Sulphate oxidation scheme now takes its oxidants from the interactive chemistry (Rae 2008)	The sulphur oxidation will now be affected by meteorology and climate
Ocean carbon cycle-DMS	DMS emission now interactively generated by the ocean biology	This important source of sulphate aerosol will now vary as climate change affects the plankton
Vegetation-Dust	Dust emissions depend on the bare soil fraction generated by the vegetation scheme	Dust production will vary as climate change affects the vegetation distribution
Dust-Ocean carbon cycle	Dust deposition affects plankton growth	The supply of nutrients to the plankton varies with the dust production. This coupling also allows geo-engineering experiments to be simulated.

Table 1.2: Summary of main changes from HadGEM2-AO to HadGEM2-ES

2. Evaluation of HadGEM2 physical components

Most of the HadGEM2 development has been carried out using the 38 level configuration. This will be the standard configuration used for all the coupled carbon cycle science and the majority of climate integrations. The L60 configuration with a higher model top and finer vertical resolution in the stratosphere will be used primarily for investigation of the role of the stratosphere in climate variability, and for coupled chemistry climate science related to the interactions between stratospheric

ozone and climate. The evaluation described in section 2 is without including the earth system components (HadGEM2-AO configuration).

2.1. Standard 38 Level model

2.1.1. Global measures of performance

A number of measures giving an overview of some general assessment of model performance against present day climate observations or reanalyses (so-called model ‘metrics’) now exist. The two measures shown here are based on the composite mean square errors of a broad range of climate variables. The first of these, the Climate Prediction Index (CPI, Murphy et al, 2004) has been used extensively through the development of HadGEM2 to track the progress against HadGEM1. Figure 2.1 shows HadGEM2 against HadGEM1 highlighting improvement (a lower score is closer to observations) in many of the variables included in the score. A second performance measure developed by Reichler and Kim, 2008 is shown in Figure 2.2. This includes a similar set of climate variables to the CPI, but is additionally useful here as it has been applied to all of the models submitted to the CMIP3 database and separates performance into the Northern and Southern Hemisphere and the Tropics (a lower score indicates better performance – see figure caption for more details). A clear improvement can be seen in HadGEM2 against HadGEM1, notably in the tropics, now putting the model in a leading position relative to the other models assessed here.

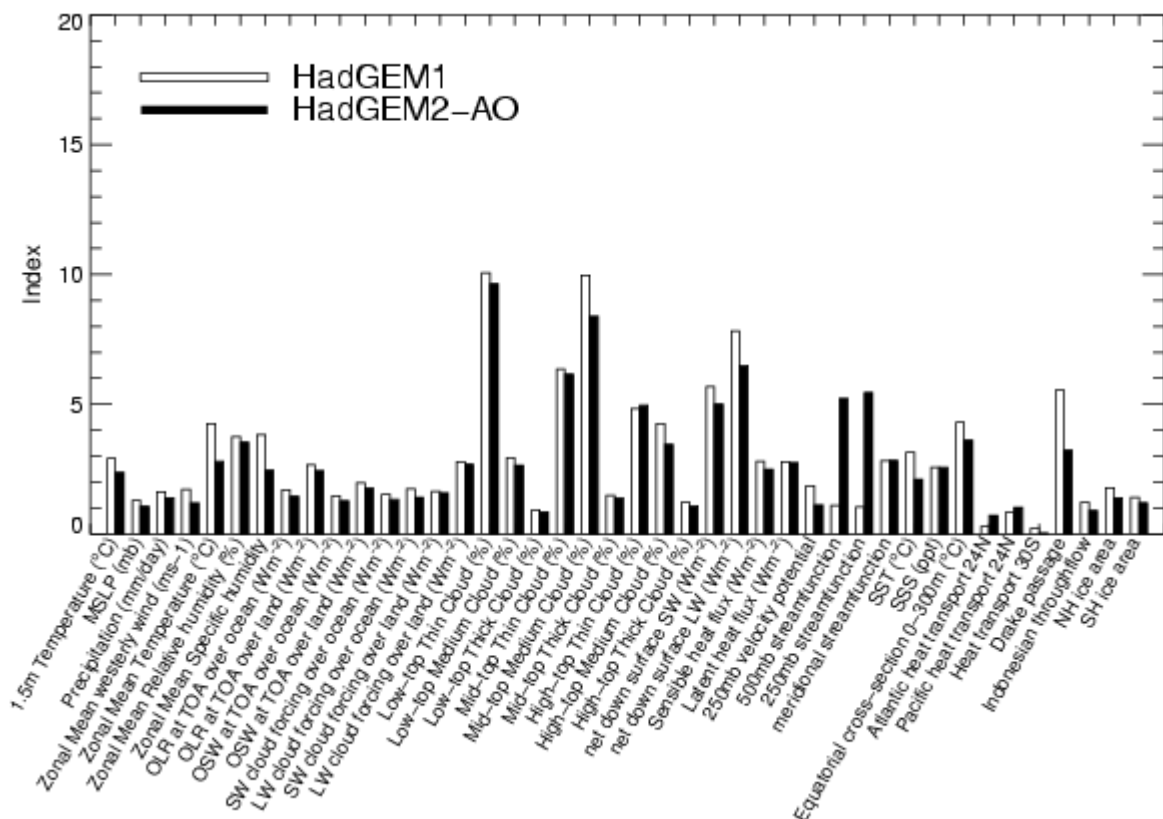


Figure 2.1: CPI (Murphy et al, 2004) for annual means of the HadGEM1 and HadGEM2 models averaged over 20 years

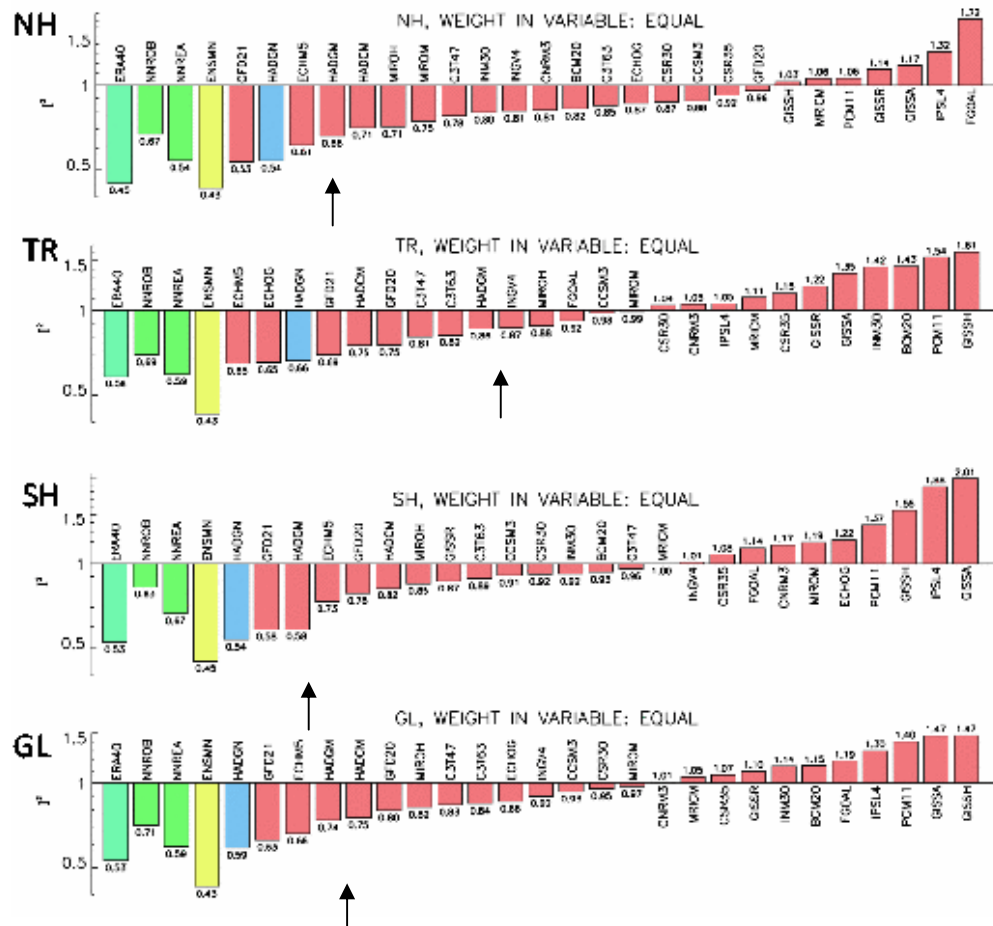


Figure 2.2: Performance measure against observations (Reichler and Kim 2008) for 3 reanalysis datasets (green bars), the mean across all models (yellow), HadGEM2 (blue) and the CMIP-3 models (red). HadGEM1 is marked with an arrow.

2.1.2. Improvements in the tropical mean-state and tropical variability errors

Global SSTs in HadGEM2 show a considerable improvement relative to HadGEM1 after around 50 years of simulation, particularly in the tropical Pacific (Figure 2.3). This improvement is robustly sustained through the length of the integration. The improvement in the mean SSTs has arisen for two main reasons; the change to the vertical diffusion in the ocean, meaning that less heat is lost from the ocean surface to the sub surface and improvements in the equatorial wind stress through the inclusion of an adaptive detrainment parameterization. HadGEM1 has substantially too strong mean wind stress in the Nino-4 region and too cold SSTs in the nino-3 region (Table 2.1) putting it well outside of the pack of CMIP-3 models for this diagnostic (Figure 2.4). HadGEM2 is now on the edge of the pack of models, showing a substantial improvement. The SST variability, (based on the standard deviations of 100 years of data from the observations and 200 years from the models) appears to be slightly better than in HadGEM1 (Table 2.1). However, analysis of the power spectrum of the Nino-3 anomaly (Table 2.1, Figure 2.5) shows that the variability in HadGEM2 seems to be on decadal timescales rather than on the 3-7 year timescale in the observations. Work is ongoing to understand the mechanisms of the triggers, development and decay of ENSO events in these models and this will be a continuing focus for HadGEM3.

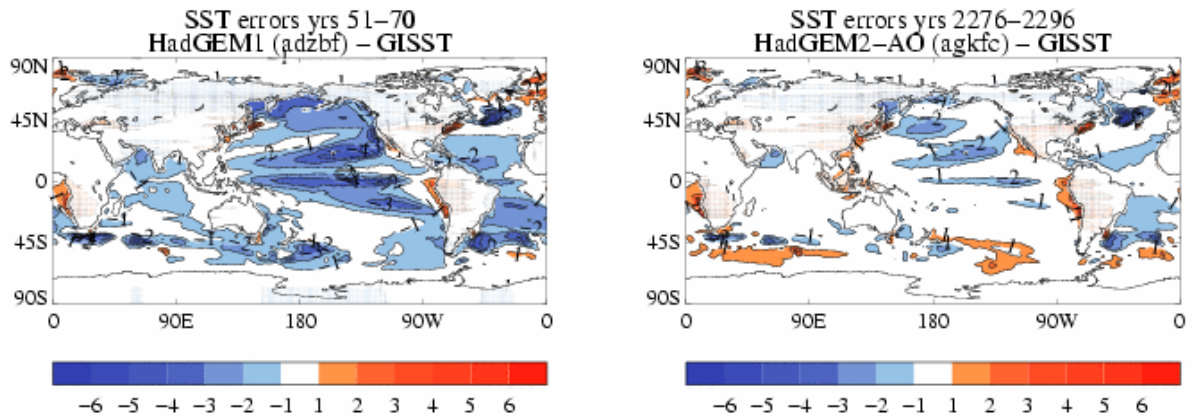


Figure 2.3 SST errors after 50-70 years of simulation. a) HadGEM1 - GISST climatology; b) HadGEM2-GISST climatology

◆s' HadGEM1
SST 23.8
TAUX -.064

✗ HadGEM2-AO
SST 24.9
TAUX -.048

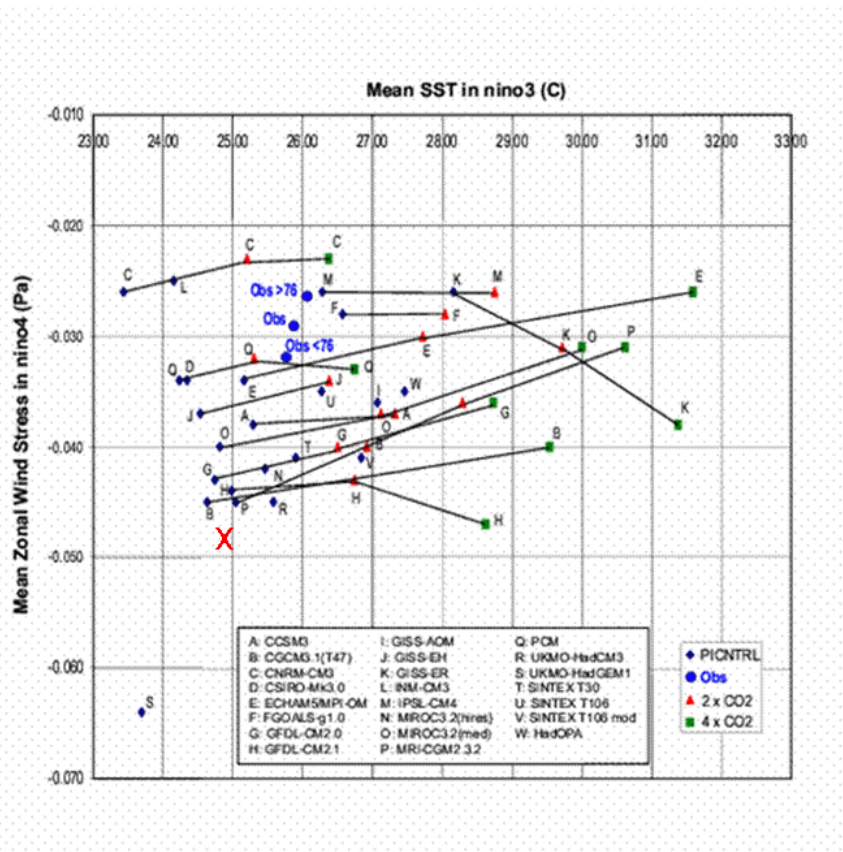


Figure 2.4: Mean SST in Nino3 (x-axis) vs mean zonal wind stress in Nino4 (y-axis) (after Eric Guilyardi, 2006) for a variety of models from CMIP3. Unperturbed models are shown by blue diamonds. HadGEM1='◆s' HadGEM2=orange cross.

A composite analysis of events identified as 'El Niño' cases (those above 1.5 SD), show that the atmospheric response during ENSO is better in HadGEM2 relative to HadGEM1 (Table 2.1, Figures 2.6). The correlation of the Nino-3 SSTs with the Southern Oscillation Index (SOI) is considerably improved and the SST and precipitation anomalies associated with these events are more similar to observations

in their magnitude and spatial extent. This is, at least in part, attributable to the improvements in the mean-state SSTs and wind stress. Understanding these improvements and the relative benefits of enhanced resolution is at the heart of work on improving ENSO within the HadGEM3 development.

	Nino-3 SD	Average Niño3 1.5σ SST period (yrs)	Mean Niño3 SST	Mean Niño4 Taux	Correlation Niño3 SST/SOI
Observations	0.80	8.3	25.9 (57yr)	-0.029 (57yr)	-0.62
HadGEM1	0.65	6.9	23.7	-0.064	-0.31
HadGEM2	0.76	9.5	24.9	-0.048	-0.45

Table 2.1: Summary statistics for ENSO mean state and variability for HadGEM1, HadGEM2 and observations (HadISST, NCEP-reanalysis, HadSLP2). The data are based on 100 years for observations (unless otherwise stated) and 200 years for the models.

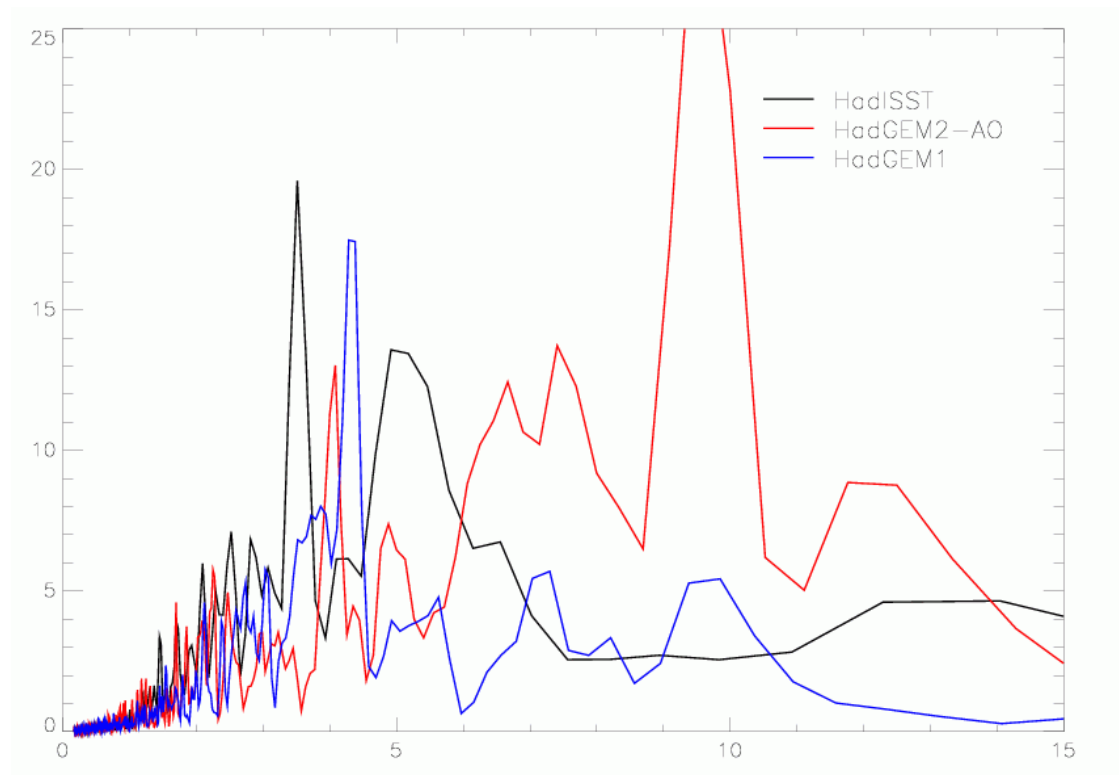


Figure 2.5: Niño-3 anomaly power spectrum

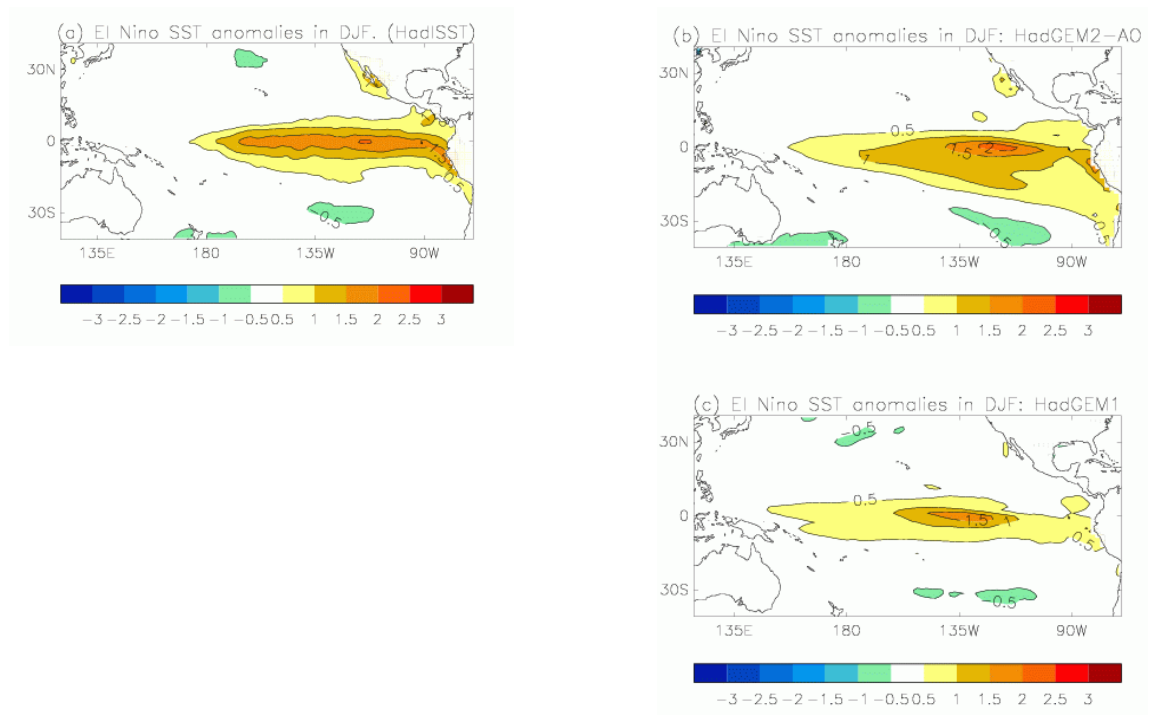


Figure 2.6: Composite SST anomalies for ‘El Nino’ events (standard deviation above 1.5x); a) HadISST (climatology), b) HadGEM2, c) HadGEM1

2.1.3 Improvements in Land surface errors

The extensive and large magnitude warm and dry biases over northern continents in HadGEM1 (e.g. Figure 2.7c) mean that when this model is coupled to dynamic vegetation, the climatological simulation of the boreal forests is very poor. This raises serious concerns about using the model to simulate Earth System feedbacks. An essential criterion for HadGEM2 is that it produces adequate vegetation to be coupled to the earth system. Generally the northern hemispheric summer warm biases over land have been reduced considerably in HadGEM2, for example over Central Asia and in North America (Figure 2.7b), reducing the errors relative to the observed climatology (Figure 2.7c,d). These improvements arise from a number of changes; the treatment of excess soil moisture in super-saturated soil layers has been changed, a background climatology of biogenic aerosols has been included, and improvement have been made to the representation of the lifetime of convective cloud. The Saharan warming comes from the adjusted soil albedo ancillary, which was a necessary retuning given the changes to the aerosols in HadGEM2. The errors are now considered small enough to be acceptable, so that in an Earth System version of the model (including dynamic vegetation) the vegetation is maintained close to observed (e.g. boreal forest in Eurasia) and Net Primary Productivity (NPP) is comparable with observations (see section 3.1).

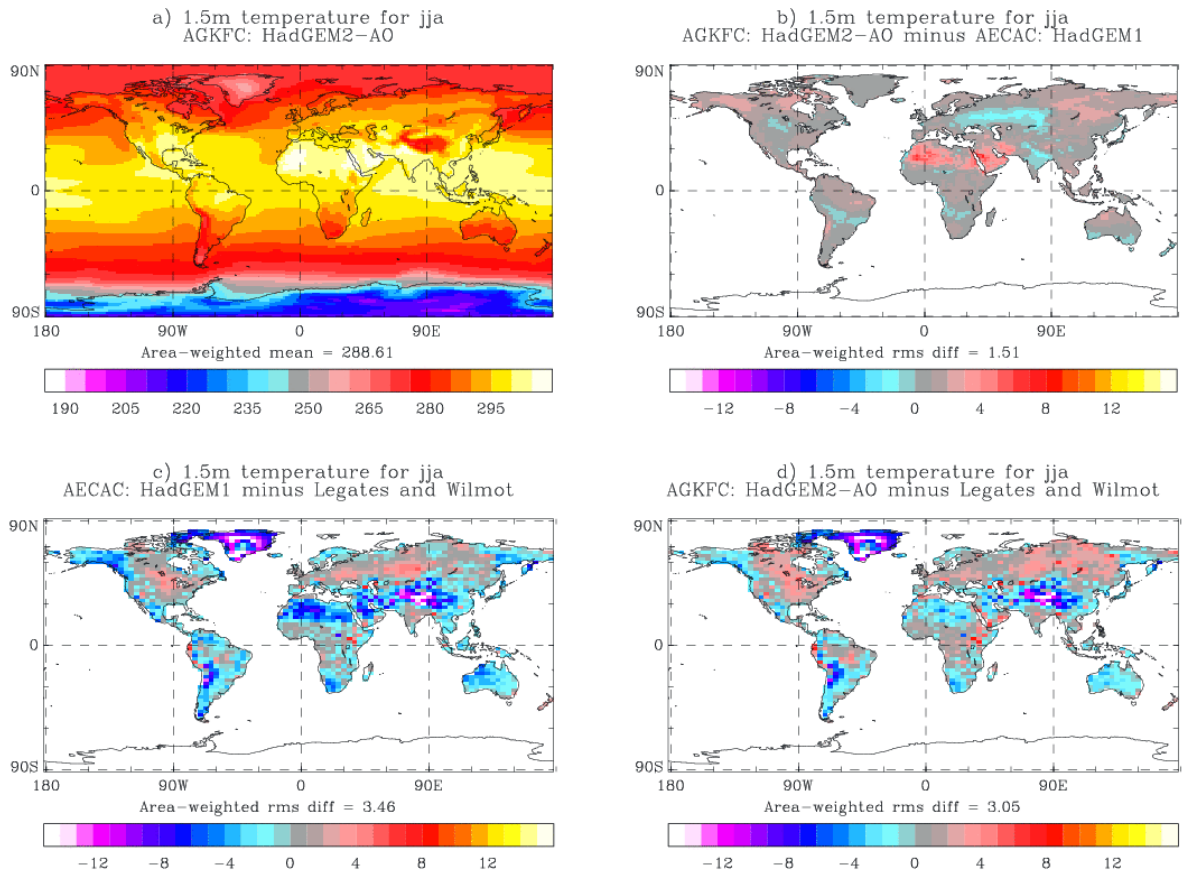


Figure 2.7: 1.5m Temperature for JJA over years . Clockwise from top left: HadGEM2-AO; HadGEM2-AO – HadGEM1; HadGEM2-AO – climatology; HadGEM1- climatology.

0800

2.2. Evaluation of vertically-extended version of HadGEM2

A vertically-extended version of HadGEM2 has been created, incorporating 60 vertical levels (compared with 38 levels in the standard version), with the additional levels mainly included above 18km. The model top has been raised from 40km to 84.5km and 13 model levels lie within this region, making the vertical resolution between 3 and 5km. Appropriate modifications to the radiation scheme and radiation spectral files are included for modelling the middle atmosphere. A source of water is introduced into the model that represents the water produced by methane oxidation in the mesosphere. There is also an additional physical parameterisation to describe the vertical transport and deposition of momentum by sub grid-scale waves (gravity waves) which is known to play an important role in the momentum balance of the mesosphere and tropical middle atmosphere. The model has an opaque lid, such that gravity waves cannot escape the top of the model and therefore they distribute momentum fluxes at the model top. This helps conserve momentum in the model.

The coupled atmosphere-ocean HadGEM2 L60 model has run for more than 50 years. A 20-year parallel atmosphere-only run has been carried out. Assessment of the global climatology using the Climate Prediction Indices (Murphy et al., 2004) shows that the L60 version has broadly similar performance to L38, particularly for the atmosphere-only version (Figure 2.8). One of the more significant (and beneficial) impacts is on the tropopause temperature and humidity, which is related to improved positioning of the tropopause in the vertically-extended model. For the coupled

models, there are some detrimental impacts in the L60 version, although these are thought to be related to an overall cooling of the climate in this model (see below).

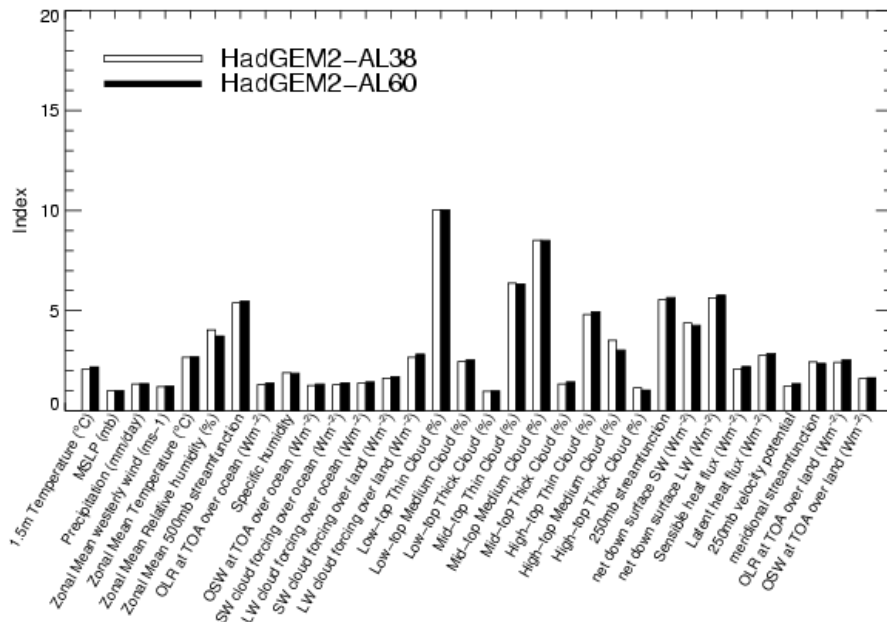


Figure 2.8: Climate Prediction Indices for atmosphere-only models HadGEM2-A L38 and HadGEM2-A L60

More detailed analysis of the atmosphere-only version shows that there are changes to the behaviour of deep convection in the L60 model. Deep convection tends to terminate at a lower level, resulting in reductions in rainfall and in high-top medium-optical depth cloud in the tropics. The impact on these cloud amounts is even more marked in the coupled model, although the impact on rainfall is less clear because of compensating changes in sea surface temperature. The reasons for the change in convective behaviour are not yet understood, although it is thought to be related to changes in the circulation brought about by the resolved stratosphere and extended model top.

The L60 model has a good simulation of the Quasi-Biennial Oscillation (QBO, Figure 2.9), with an average period of 29.2 months, a westerly phase of 15.6 ms^{-1} and an easterly phase of -25.3 ms^{-1} in good agreement with observations. The tape recorder signal in equatorial upper atmospheric moisture is weaker than in observations, but the spin-up in moisture levels is much reduced compared with earlier in the development of the L60 model.

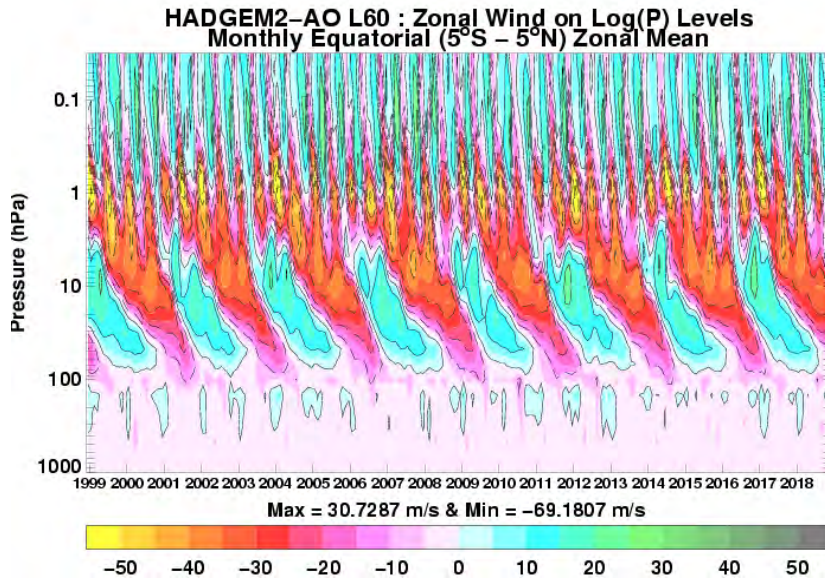


Figure 2.9: Hovmoller plot of monthly equatorial zonal wind profiles showing the quasi-biennial oscillation (QBO)

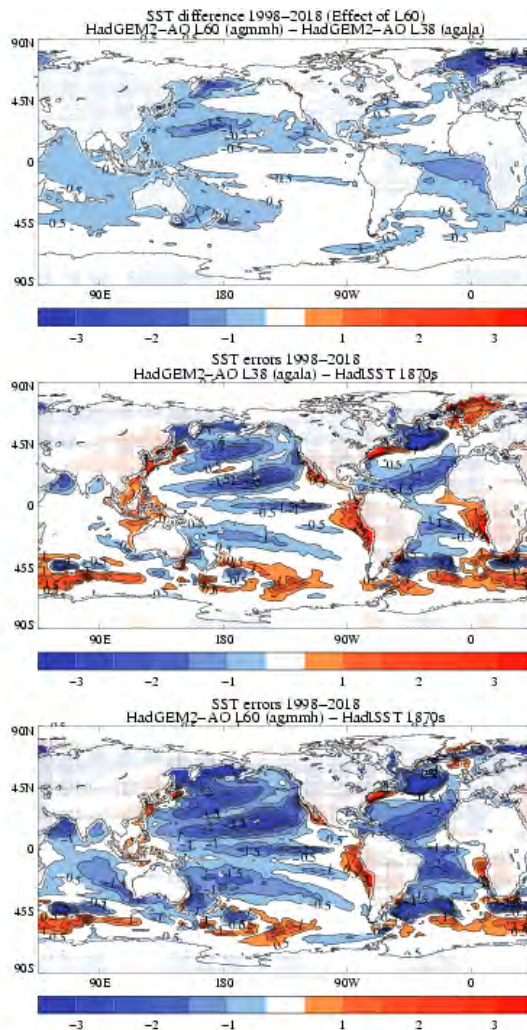


Figure 2.10: (a) Sea surface temperature (SST) differences in HadGEM2 (L60 - L38); (b and c) SST errors (compared with observations) in (b) HadGEM2 L38 and (c) HadGEM2 L60

The coupled atmosphere-ocean HadGEM2 L60 has now run stably for >50 years. As a result of the modifications to the radiation scheme for the middle atmosphere (mentioned above), the top-of-atmosphere (TOA) radiation at the start of the run is slightly out of balance (and negative compared with L38). The model spins-up to TOA equilibrium rapidly, but with ocean temperatures half a degree cooler than at L38. Of particular note is the cooling in the far North Atlantic (Figure 2.10), leading to increased sea ice extent. This is possibly also important in terms of an increase in the Atlantic Meridional Overturning Circulation (MOC) to ~25Sv. This is significantly higher than in the L38 version (around 20Sv) and excessive compared with observations. It is possible that this will be reduced following tuning of the TOA radiation.

2.3. Aerosols in HadGEM2

Seven aerosol species are available in HadGEM2. They are sulphate, fossil-fuel black and organic carbon, sea-salt, mineral dust, biomass-burning, and biogenic aerosols. Aerosols scatter and absorb solar and terrestrial radiation (direct effect), and provide the cloud droplet number (indirect effect). In HadGEM2-ES, aerosols are coupled with other components of the model, such as the vegetation scheme and the ocean model.

Aerosol schemes have been revised since HadGEM1. Most changes are detailed in the Hadley Centre technical note by Bellouin et al. (2007). More recent changes are summarised here.

2.3.1. Changes to sulphate aerosols

The sulphate aerosol scheme in HadGEM1 is described by Jones et al. (2001), and the changes introduced for HadGEM2 are described by Bellouin et al. (2007). Although those changes have significantly improved the performance of the sulphur cycle in the model, sulphate aerosol concentrations remain underestimated compared to observations, particularly over northern continents in winter. One reason for this is the absence of aqueous oxidation of dissolved SO₂ by dissolved ozone (O₃) to produce dissolved-mode sulphate aerosol in cloud droplets. This reaction has therefore been introduced in HadGEM2-ES.

In reality, the rate of this reaction is highly dependent on pH; however, a representation of such a dependence would be extremely difficult in the current model, and a very simple treatment is therefore used. The reaction of SO₂ with O₃ is assumed to proceed in a particular gridbox only if the mass-mixing ratio of H₂O₂ is smaller than that of SO₂, as otherwise all SO₂ in the gridbox would be removed by the reaction with H₂O₂ and none would be available for oxidation by O₃. This is a consequence of the way the SO₂+H₂O₂ reaction is parameterised in the model (see Jones et al., 2001, for further details). In addition, the reaction only proceeds if the O₃ mass-mixing ratio is greater than 16 parts per billion. If these two conditions are satisfied, then the SO₂+O₃ reaction is assumed to proceed at the same rate as the SO₂+H₂O₂ reaction (see Jones et al., 2001). All sulphate produced by these two aqueous reactions is transferred to the dissolved mode.

When the reaction with O₃ is included in the model, modelled sulphate concentrations are significantly improved when compared to observations, particularly over Europe

in winter. Figure 2.11 shows a comparison of modelled sulphate with observations from the EMEP network in Europe (www.emep.int) for January (Hjellbrekke et al. 2002). Figure 2.11 clearly shows that, when oxidation by ozone is introduced, the model results match observations much more closely. This change therefore goes some way towards solving a major discrepancy in previous versions of the model.

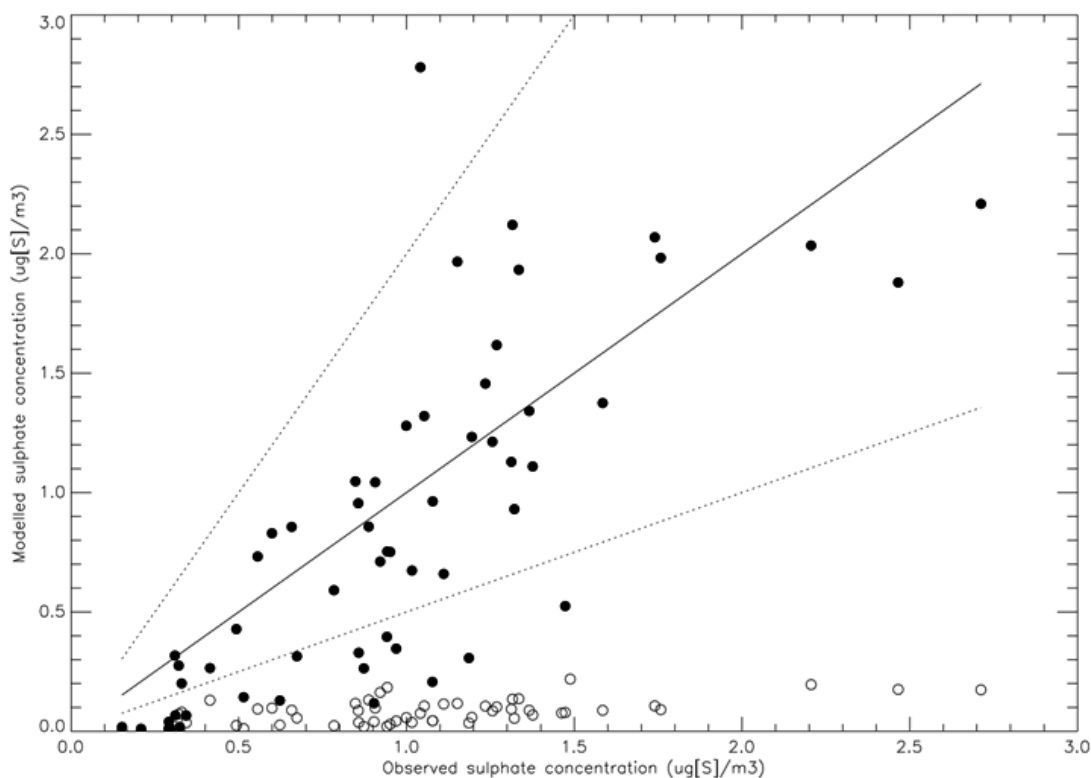


Figure 2.11. Comparison of modelled and observed sulphate concentrations (μg of sulphur per m^3) over Europe in January. Values plotted are means of the four January monthly means for 1995, 1996, 1997 and 1998. Open circles show the model without aqueous reaction between dissolved sulphate and ozone. Closed circles show the model with that reaction. The solid line is the 1 to 1 line; dashed lines are the 1 to 2 and 2 to 1 lines.

2.3.2 Addition of fossil-fuel organic carbon aerosols

Fossil-fuel organic carbon (FFOC) is an important anthropogenic species in industrialised regions and has been added to HadGEM2 in the earth system configuration. The FFOC scheme is similar to that for biomass-burning aerosols (Davison et al., 2004). Emissions from fossil-fuels and biofuels are taken from the AeroCom project (Dentener et al., 2006). FFOC aerosols are emitted into a fresh, mode which ages to a larger aged mode with an e-folding time of 1 day. Both modes experience hygroscopic growth due to water uptake. A fraction of the aged-mode aerosol is incorporated into cloud droplets. FFOC aerosols experience dry and wet deposition. The fresh and aged modes scatter and absorb radiation (direct effect) and the in-cloud mode affects the cloud droplet size (indirect effect).

In the absence of specific measurements, organic carbon aerosol size distribution, density, and hygroscopic growth factors are assumed to be the same as those of biomass-burning aerosols Bellouin et al. (2007). The real part of the complex refractive index is also equal to that of aged biomass-burning aerosols. The imaginary part is assumed to be wavelength-independent and is set to 0.06. FFOC aerosols are

more scattering than biomass-burning aerosols and more absorbing than ammonium sulphate aerosols.

In Figure 2.12, we compare total particulate organic matter (POM) with measurements. Total POM consists of biomass-burning, FFOC and natural biogenic components. Modelled concentrations compare within a factor of two against measurements over Europe and North America, with a tendency towards underestimation. FFOC aerosols have a lifetime of 5.2 days resulting in an annual global mean burden of 0.19 Tg. This is in agreement with other global modelling studies (e.g. Reddy et al., 2005).

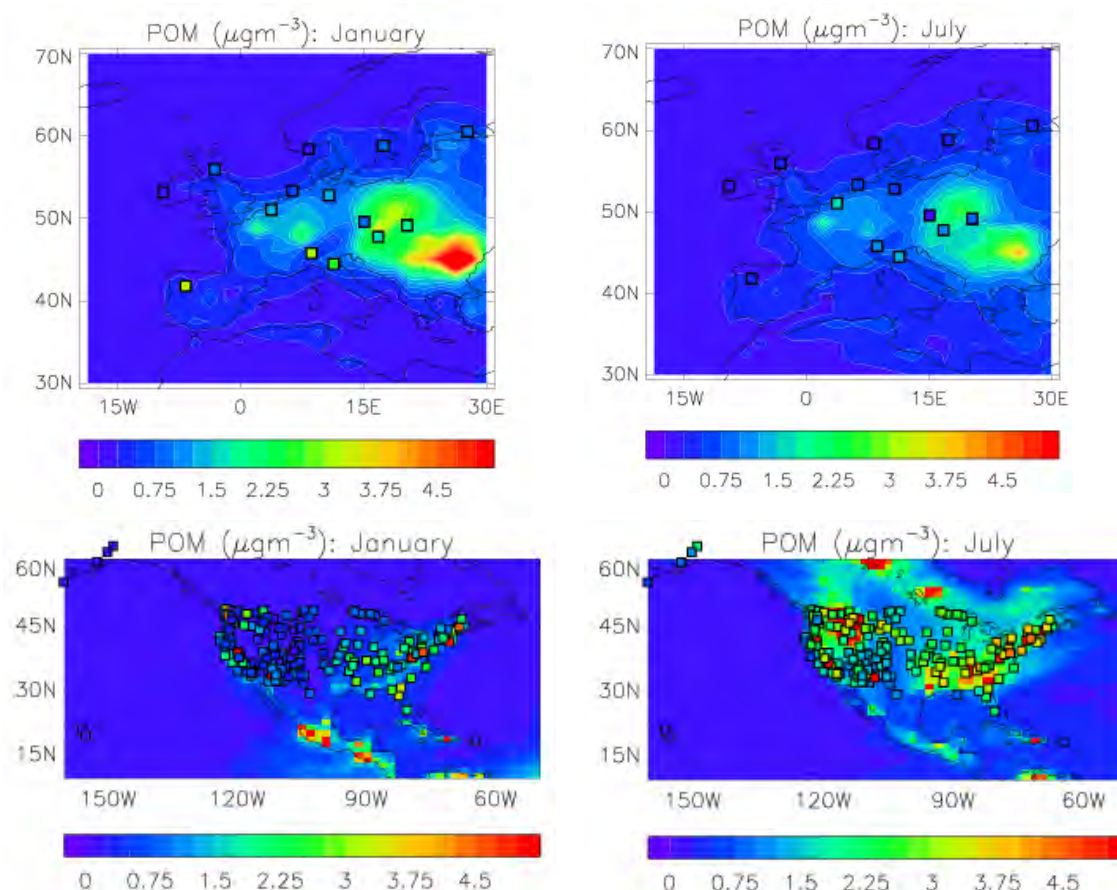


Figure 2.12 Comparison of modelled surface concentrations of particulate organic matter ($\mu\text{g m}^{-3}$) in HadGEM2 with measurements from EMEP (Europe, top panels; Hjellbrekke et al. 2002) and IMPROVE (North America, bottom panels; Debell et al. 2006) networks. Measurements are overlaid as coloured squares over the modelled distributions. Left column is for January, right column is for July.

2.3.3 Changes to mineral dust aerosols

Mineral dust aerosol has been built into the standard climate model for the first time at HadGEM2. Particles are released from bare soil surfaces when friction velocity exceeds a size-dependent threshold, and form a horizontal flux close to the ground. A fraction of this flux is then lofted upwards to produce a vertical flux. The dust is transported throughout the atmosphere, being removed by dry and wet deposition processes and affecting both shortwave and longwave radiative fluxes. The deposition

of dust to the ocean provides a major source of iron to phytoplankton and may thus affect the carbon cycle.

The dust model in HadGEM2 is based on that created for use with HadAM3 (Woodward, 2001), but with significant improvements to the dust emission scheme. The values of the impact threshold friction velocity are derived from the data of Bagnold (1941); this is more physically realistic than the fluid threshold values previously used. Parameterisation of the effect of soil moisture is based on the algorithm of Fecan et al. (1999), which is better validated and more sophisticated than the method used with HadAM3. Both friction velocity and soil moisture terms are adjusted to correct for the effects of spatial and temporal scaling. The modelled horizontal flux includes a wide size range of particles from .06 to 2000 microns in 9 bins, which is also an improvement on the more limited range previously used. The total horizontal flux in each bin and the relation between total horizontal and vertical fluxes were calculated according to the widely used model of Marticorena and Bergametti (1995). Vertical flux is calculated for particles up to 60 microns in 6 bins, the size distribution following that of the horizontal flux in this range.

As dust production is highly sensitive to climate and almost no data on pre-industrial dust concentrations are available, the evaluation of the dust scheme has been carried out using 10 years of data from a present-day, atmosphere-only HadGEM2 experiment. The mean annual cycle of near-surface dust concentration has been compared with observations at 18 sites from the University of Miami network of stations. Generally good agreement between the model and observations is seen, particularly for stations affected largely by Saharan and Australian dust. Comparison of aerosol optical depths with observations at 3 AERONET stations in dust-dominated regions of North Africa and the Middle East shows that the model also successfully simulates the annual cycle of dust AODs in that region. Figure 2.13 shows examples of results from this evaluation.

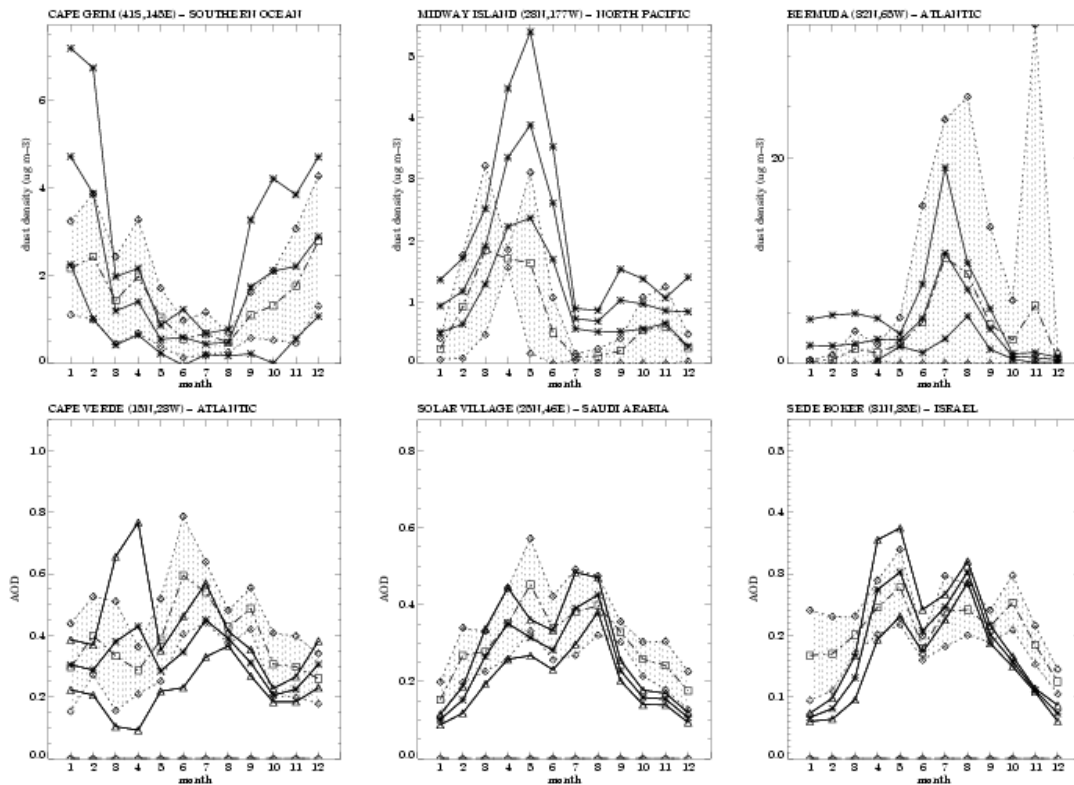


Figure 2.13. Comparison of HadGEM2 and observed annual cycle of mineral dust fields. Observational multi-annual means are indicated by squares joined by dashed lines, and shaded areas show the observed mean \pm one standard deviation. Solid lines indicate model decadal means and model means \pm one standard deviation. The top three figures show near surface concentrations at stations of the University of Miami network. The bottom three figures show total aerosol optical depth at 440nm at three AERONET stations.

2.3.4 Aerosol optical depth and radiative forcing

Changes to aerosol representations since HadGEM1 have a significant impact on aerosol optical depths (AODs). The AOD is a measure of the column-integrated extinction of radiation by aerosols at a given wavelength. It is routinely retrieved by satellite instruments. As presented in Bellouin et al. (2007), HadGEM2 simulates the global distribution of the AOD well. Here, we focus on the improvement since HadGEM1. Figure 2.14 is a Taylor diagram (Taylor, 2001) assessing the performance of the AOD simulation against measurements by ground-based sun-photometers of the Aerosol Robotic Network (AERONET). AERONET monthly means are computed from quality-assured daily measurements at $0.44 \mu\text{m}$ made in the period 1998-2002 at sites mostly located in Europe and North America, with fewer sites in Asia and Africa. Modelled AODs at $0.44 \mu\text{m}$ were taken from the grid-box containing the AERONET site for both HadGEM1 and HadGEM2-A. The improvement since HadGEM1 is obvious. Correlations with AERONET have increased and are now larger than 0.6 for all months. Normalised standard deviations are close to 1 for 7 months, suggesting that the model represents well the geographic variability of AOD. The variability is underestimated for the period January to April, and overestimated in July.

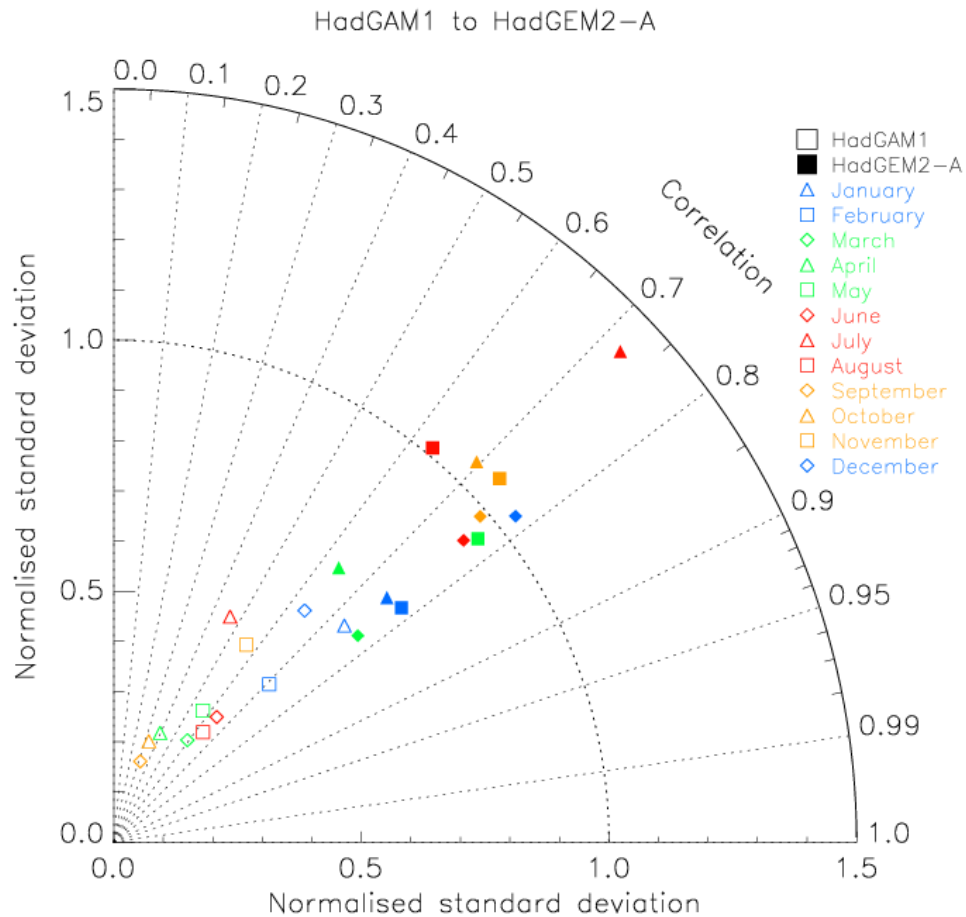


Figure 2.14. Taylor diagram summarising the comparison of monthly total aerosol optical depths at $0.44 \mu\text{m}$ in HadGAM1 (open symbols) and HadGEM2 (closed symbols) against AERONET measurements. Note that correlations are given on a non-linear scale. A perfect match of the measurements would yield a point with a normalised standard deviation of 1 and a correlation coefficient of 1.

In HadGEM2, including only the changes described in Bellouin et al. (2007), the total (direct and indirect) forcing due aerosol between 1860 and 2000 was -1.44 Wm^{-2} . Adding fossil-fuel organic carbon aerosols increased the forcing to -1.53 Wm^{-2} . Adding changes to the sulphur cycle as described in section 2.3.1 decreased the forcing to its current value of -1.12 Wm^{-2} , as changes increase the aerosol loading in the source regions, but decrease the long-range transport and opportunities of interacting with clouds.

3 Evaluation of the Earth System components

3.1 Large-scale hydrology scheme.

A large-scale hydrology module (LSH) has been introduced into HadGEM2 in order to improve the soil moisture, and hence the vegetation distribution, and provide additional functionality such as simulation of wetland area required for interactive methane emissions.. It is an addition to the physical components described and evaluated above in section 2. LSH (Clark and Gedney 2008; Gedney and Cox 2003) is

based on the TOPMODEL approach (Beven & Kirkby, 1979) whereby soil moisture and runoff are affected by local topography as well as meteorology, vegetation and soil properties. In the standard scheme (Essery et al 2003) water was lost out of the bottom of the soil column through gravitational drainage. In LSH the hydraulic conductivity decreases with depth below the root zone allowing a saturated zone to form. Water is lost through lateral sub-surface flow within this saturated zone. Hence LSH tends to produce more soil moisture in the deeper layers especially when there is relatively little topography (less lateral flow) and when there is partial freezing. When there is partial freezing deep in the soil the unfrozen soil moisture is clearly lowered. Gravitational drainage tends to lead to a small vertical gradient in unfrozen soil moisture. Hence the unfrozen soil moisture contents in the shallower layers are all effectively limited by the extent of soil moisture freezing in the deep layer.

A sub-grid distribution of soil moisture/water table can be inferred from the sub-grid scale distribution in topography and mean soil moisture. Hence partial inundation within each grid box may occur enhancing surface runoff. This can also be used to diagnose a wetland fraction for calculating interactive wetland emissions (Gedney et al. 2004), and is used by the chemistry scheme (section 3.4.1).

3.2. Evaluation of terrestrial carbon cycle components.

Throughout this section we analyse the simulation of the terrestrial carbon cycle by HadGEM2 in a pre-industrial control phase, with atmospheric CO₂ held fixed at 290 ppmv. The main aim is to assess how well the model performs and whether it is fit for purpose as an Earth System model, but we also make use of a comparison against HadCM3LC simulations as a benchmark and, where available, some data from the range of C4MIP coupled climate-carbon cycle models (Friedlingstein et al., 2006). More details of the simulation of the terrestrial carbon cycle by HadGEM2 can be found in the assessment report of Jones et al. (2008).

3.2.1. Vegetation cover.

The vegetation model used in HadGEM2 is TRIFFID (Cox, 2001), the same as used in HadCM3LC. It simulates the growth and competition of 5 plant functional types (broad-leaved and needle-leaved trees, C3 and C4 grasses and shrubs). When run to steady state the vegetation simulation of HadGEM2 compares favourably with observed land cover maps and is generally a little better than that simulated by HadCM3LC. The observed climatology here is generated by adjusting the IGBP present day vegetation dataset to be consistent with a historical reconstruction of 1860 vegetation (Klein Goldewijk, 2001) as described by Betts et al (2007). No prescribed land cover change is included in HadGEM2 at this stage, but an agricultural mask is applied to prevent tree and shrub growth in agricultural regions. In the case shown here the agriculture is representative of present day and is static in time. A land-cover change scheme is being implemented and will be used with dynamic land-use in transient simulations.

Figure 3.1 shows the climatological and simulated total tree cover and bare soil. For broadleaf trees HadGEM2 is generally a little better than HadCM3LC, especially in temperate latitudes where it correctly simulates some coverage in the mixed forest areas to the southern edge of the boreal forest zone. In the tropics both GCMs have a

tendency to simulate too much extent of tropical forest but HadGEM2 has an improved coverage in the north east of Brazil where HadCM3LC has a gap in the forest. For needleleaf tree HadGEM2 simulation is similar to that of HadCM3LC. Neither model correctly simulates the area of cold-deciduous larch forest in east Siberia whose phenology is not well represented in TRIFFID. HadGEM2 now also simulates a patch of spurious forest in the Himalayan region which in reality should be grass and shrub. Overall HadGEM2 does a good job at simulating the global distribution of trees.

Grass and shrub are generally simulated better than in HadCM3LC which had much too great coverage in the high latitudes. HadGEM2 now simulates slightly too little in the far north of Siberia and North America, but the overall distribution is better. This comes though at the expense of simulating too little shrub and too much grass. Inclusion of an agricultural mask to prevent trees growing in areas of present day agriculture results in the model being able to represent well the main agricultural regions of North America, Europe and Asia. The HadGEM2 simulation is now better in temperate zones and central Africa but, as before, there is too little coverage in Australia.

Bare soil is diagnosed from the absence of simulated vegetation. HadGEM2 captures the main features of the world's deserts, and is better than the previous simulation of HadCM3LC except in Australia where it now simulates too great an extent of bare soil. The main tropical deserts are captured as before, but now HadGEM2 also simulates better representation of bare soil areas in mid-latitudes and the south western USA. As before, the simulated Sahara/Sahel boundary is slightly too far south. Along with Australia, there is also too much bare soil in northern Siberia where the observed cover of around 50% is simulated above 80%.

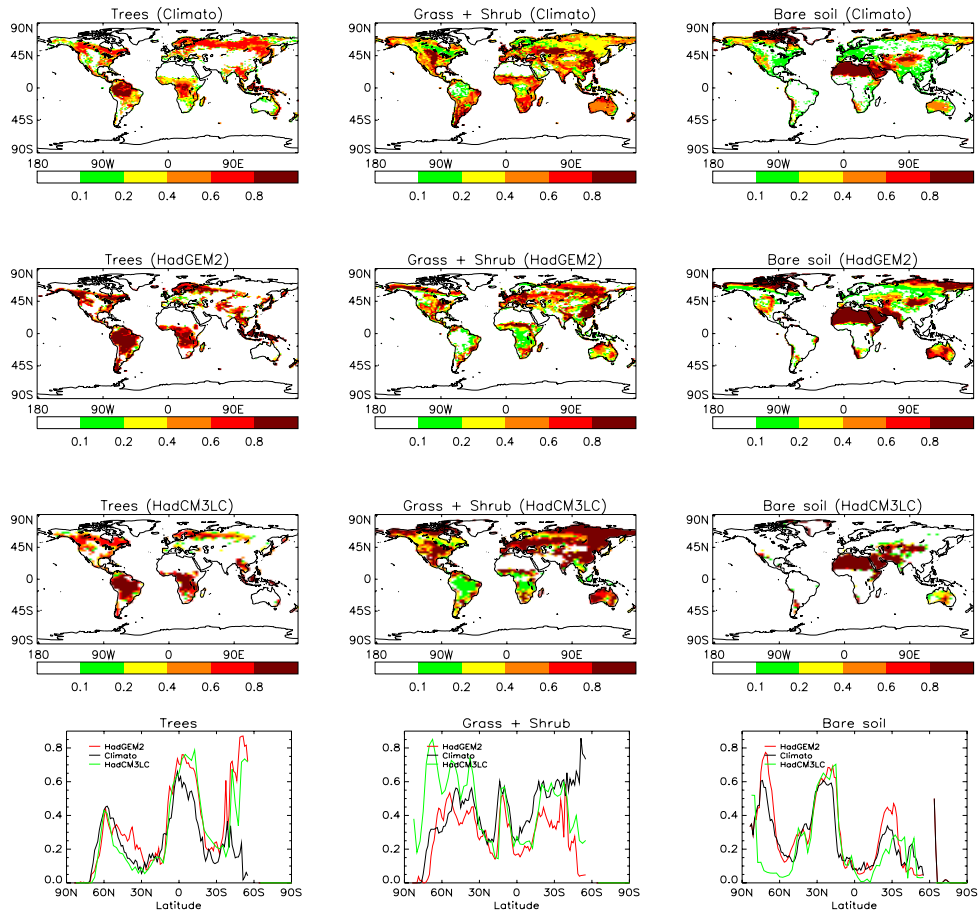


Figure 3.1. IGBP Climatology and HadGEM2 simulation of tree cover (defined as the total of both broadleaf and needleleaf tree), grass, shrub and bare soil.

3.2.2. Simulation of terrestrial carbon stores.

A primary reason for including a vegetation model in HadGEM2 is to simulate the global distribution of fluxes and stores of carbon. Organic carbon is stored in the soil when dead litter falls from vegetation, either as dropped leaves or branches or when whole plants die. It is returned to the atmosphere as soil (or heterotrophic) respiration when soil organic matter is decomposed by microbes. In HadCM3LC soil carbon was simulated as a single pool with a single turnover time. In HadGEM2 we have implemented the 4-pool RothC soil carbon model (Coleman and Jenkinson, 1999) which simulates differentiated turnover times of four different pools of soil carbon ranging from easily decomposable plant matter to relatively resistant humus. Multi-pool soil carbon dynamics have been shown to affect the transient response of soil carbon to climate change (Jones et al. 2005). Although each RothC pool currently has the same sensitivity to soil temperatures and moisture there is the ability to allow the model to enable different sensitivities for each pool as suggested by Davidson and Janssens (2006).

The global total soil carbon is estimated as about 1400-1500 GtC but with considerable uncertainty. HadGEM2 simulates 1204GtC globally, HadCM3LC simulates 1173 GtC. Considering that some of the observed estimate will be more inert carbon (not represented in our models) and that the models are not yet designed

to simulate the large carbon accumulations in organic peat soils, it may be expected that the simulations underestimate the global total.

Figure 3.2 shows the climatological and simulated distribution of soil carbon. Both HadGEM2 and HadCM3LC models do a reasonable job at representing the main features with HadGEM2 improved in the extra-tropics but now under-representing the observed soil carbon in the tropics. Insufficient vegetation in Siberia and Australia leads inevitably to too little soil carbon in those regions, which previously had too much.

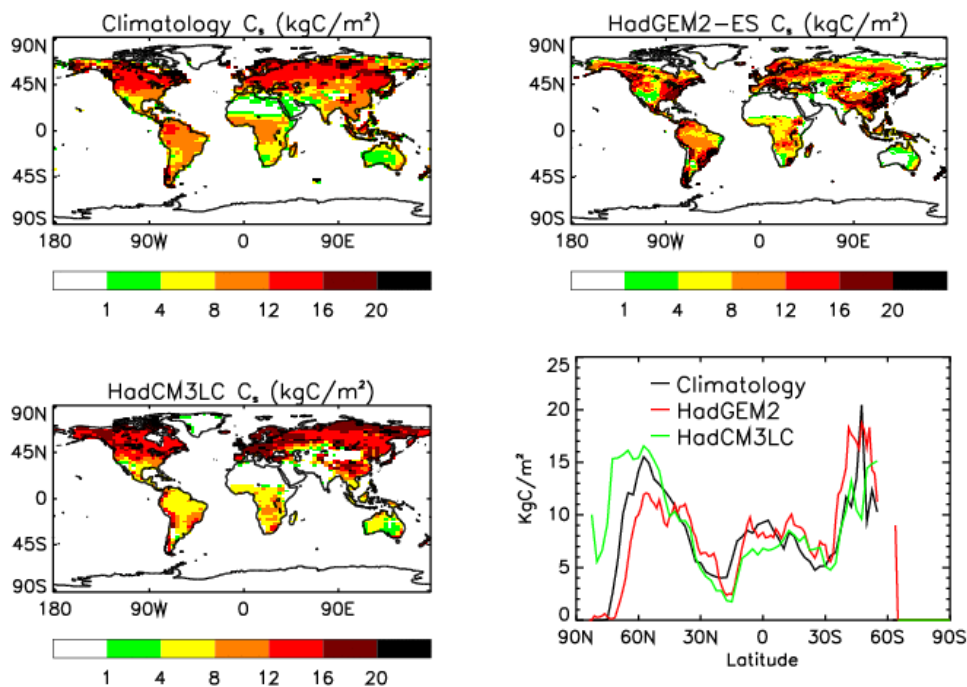


Figure 3.2. Climatological (Zinke et al., 1986) and simulated (HadGEM2 top right, HadCM3LC bottom left) soil carbon distributions. Bottom right shows a comparison of the zonal means of these distributions.

Both models do a reasonable job at representing the main features of global vegetation carbon storage although they have a tendency to underestimate biomass in regions of low amounts. HadGEM2 has an improved simulation of the biomass per unit area of the Amazon forest which was previously a little low in HadCM3LC, but the zonal mean shows that it now overestimates the total tropical biomass due to having too great an extent of forest. Similarly, areas of too low biomass (e.g. Northern latitudes) coincide with areas where we have already noted errors in the simulated distribution of vegetation such as Siberia. Globally, vegetation carbon is estimated to be between 450 and 550 GtC but this has very large uncertainty with upper and lower ranges estimated at around 270 GtC and 900 GtC. HadGEM2 now simulates 599GtC compared with 496 GtC in HadCM3LC – both well within a realistic range. Much of this over-estimate is due to simulation of too great an extent of tropical forest. The main areas of disagreement between observed and simulated biomass are due to errors in simulated vegetation cover, but there also exist errors in biomass for each vegetation type such as slight over prediction of biomass in tropical trees and under prediction of biomass in conifers and grasses

3.2.3. Simulation of vegetation productivity.

Global carbon stores are determined by the fluxes of carbon into and out of the vegetation/soil system. The fluxes “in” are due to vegetation productivity, and the fluxes “out” due to vegetation and soil respiration. Productivity is frequently expressed as gross primary production (GPP) which is the total carbon uptake by photosynthesis, and net primary production (NPP) which is the difference between GPP and plant respiration (carbon released by the plant’s metabolism). The carbon cycle is closed by the release of soil respiration – decomposition of dead organic matter. In the absence of a fire model the net flux (net ecosystem exchange, NEE, or net ecosystem productivity, NEP) is therefore given by GPP-total respiration.

A comprehensive tuning of the terrestrial ecosystem parameters has been undertaken to improve the carbon fluxes compared to HadCM3LC. For HadGEM2 we increased the top leaf nitrogen concentrations. The values adopted by HadCM3LC were generally too low. The Q10 temperature response function of soil heterotrophs was kept from HadCM3LC, rather than using the generic function in RothC (which leads to too high peak soil respiration in mid-summer). In addition the soil respiration is now driven by soil temperatures from the second soil layer instead of the first layer as in HadCM3LC, as most of the decomposable soil carbon would be on average at this depth. This leads to a damped amplitude of seasonal soil temperatures, and thus reduced seasonality in soil respiration. The response of soil respiration to moisture is represented by the total soil moisture (frozen plus unfrozen), compensating for a cold bias in high latitude winter temperatures. Finally seasonality in leaf phenology of temperate ecosystems, and thus seasonal plant productivity, is improved by delaying the onset of the growing season relative to HadCM3LC.

Component carbon fluxes are hard to measure directly, but some datasets do exist. Here we have used the ISLSCP climatology (The International Satellite Land Surface Climatology Project, Cramer et al., 1999), a global, gridded product derived from the mean NPP simulations of 17 terrestrial ecosystem models driven by observed climate, and flux tower data for 20 sites representative of major northern hemisphere biomes were obtained from the EUROFLUX (Valentini 2002) and AMERIFLUX (<http://public.ornl.gov/ameriflux/>) projects.

Figure 3.3 shows the zonal distribution of global NPP from several model configurations compared with that from the ISLSCP model-mean dataset (Cramer et al., 1999). The ISLSCP dataset also provides the standard deviation of model results about the mean, and a comparison of the dataset with site level observations shows that ± 3 standard deviation is an appropriate estimate of uncertainty.

The figure shows separate lines for HadGEM2 with (-ES) and without (-AO) dynamic vegetation. The -ES version has a dynamic vegetation distribution rather than a climatology, but more importantly many of the vegetation growth parameters have been tuned between HadGEM2-AO and HadGEM2-ES. The comparison shows HadGEM2-ES has the best simulation of global NPP. In the far north, above 65N, both HadGEM2-ES and HadGEM2-AO have too little productivity, but generally show better mid-latitude productivity than HadCM3LC whose values were much too

high. South of 40N however, HadGEM2-AO has too low productivity whereas HadGEM2-ES is much closer to the observed estimate. HadGEM2-ES is the only model to closely match the climatology in both tropics and extra-tropics.

HadCM3LC generally under predicts the amplitude of the seasonal cycle of NEP at monitoring stations whereas HadGEM2 performs much better. Figure 3.4 illustrates the flux components at one of these sites, Harvard Forest. At Harvard Forest, HadCM3LC even misses the summer draw down due to too early onset of growth and too large summer respiration. Both of these tendencies have been addressed in HadGEM2 which now better simulates both component fluxes and the net seasonal cycle. Both models are better at reproducing the seasonality of fluxes in forested ecosystems. Results are worse at sites representing water limited ecosystems, e.g. grasslands, Mediterranean ecosystems. HadGEM2 has an improved phase in the seasonal cycle of GPP compared with HadCM3LC which consistently simulated too early onset of spring uptake, and has an improved peak-season amplitude. In contrast, the heterotrophic respiration was too peaked in HadCM3LC. This has been flattened in HadGEM2, leading to total respiration in better agreement with the Harvard Forest. The combination of a more peaked GPP and a less peaked respiration gives a much better simulation of the NEP in HadGEM2. Both improved treatment of penetration of light through the canopy (Mercado et al, 2007) and tuning of the vegetation to delay the onset of the growing season have contributed to the improved simulation of photosynthesis. Across the flux sites considered, HadGEM2-ES has a lower normalised RMS error than HadCM3LC for GPP, respiration and NEP.

We conclude that for both the simulation of the seasonal cycle of component carbon fluxes and the global distribution of simulated NPP, HadGEM2 performs better than previously seen in HadCM3LC.

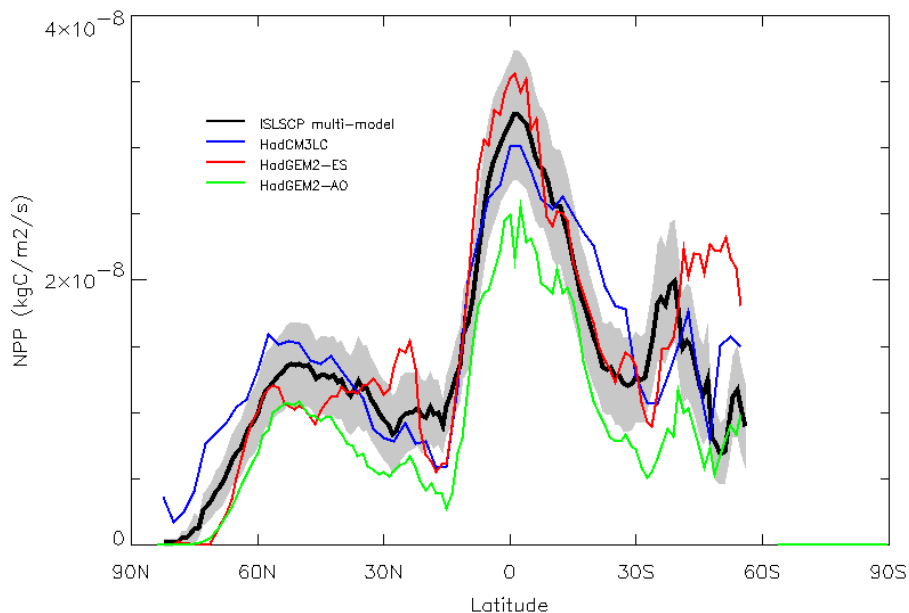


Figure 3.3. Zonal mean distribution of NPP from 3 models (HadGEM2 with fixed vegetation in green, HadGEM2 with dynamic vegetation in red and HadCM3LC in blue) compared with an estimate of global NPP from the ISLSCP model database (black) with ± 3 standard deviations plotted in dashed

lines and shaded. Simulations under pre-industrial conditions have been scaled up by 13% to allow for the effect of increased CO₂ at present day.

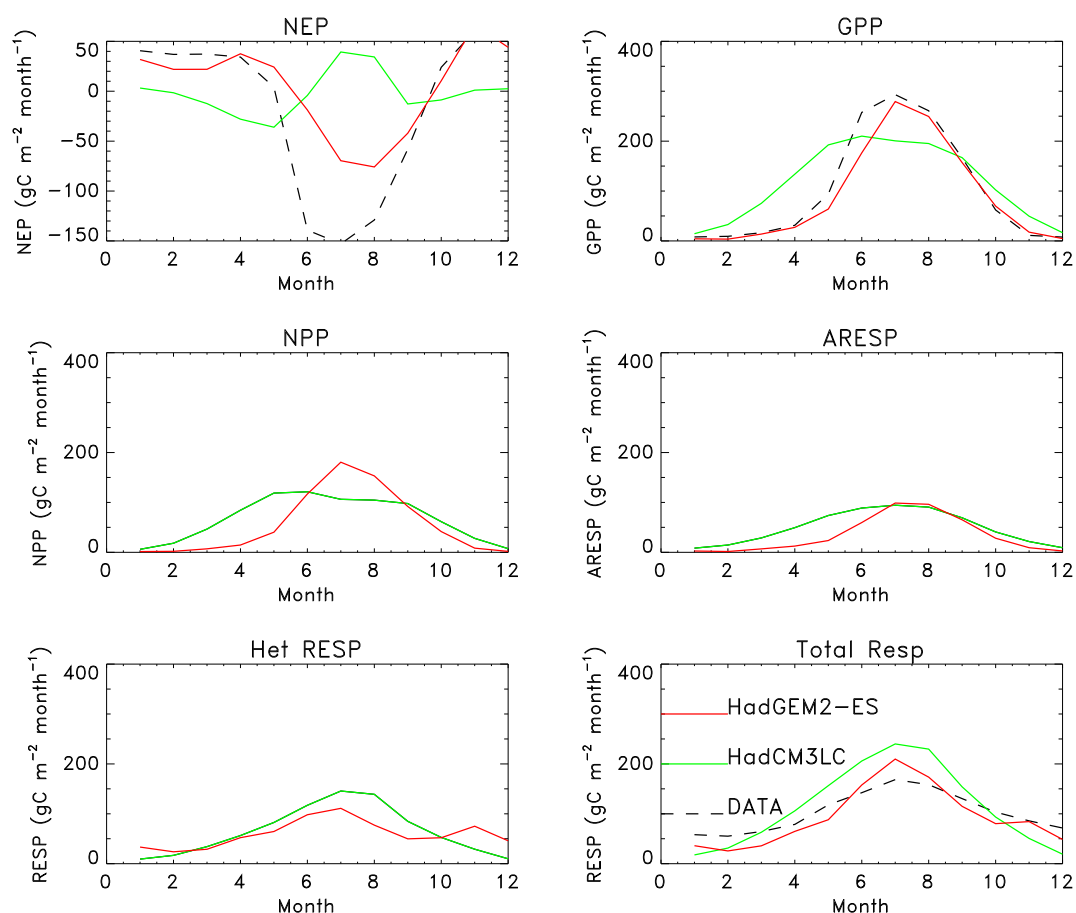


Figure 3.4. Observed and simulated carbon fluxes at Harvard Forest site, USA. HadGEM2-ES (red), HadCM3LC (green).

3.3 Ocean biogeochemistry

Ocean biogeochemistry in HadGEM2 consists of an ecosystem model and related sub-models for seawater carbon chemistry and the air-sea transport of CO₂, the cycling of iron supplied by atmospheric dust, and the production and sea-to-air transfer of dimethylsulphide (DMS).

The ecosystem model used is the Diat-HadOCC model, a development of the previous HadOCC model (Palmer and Totterdell 2001) that splits the phytoplankton compartment into “diatoms” and “other phytoplankton”. Diatoms require silicate to form their shells, are very sensitive to iron-limitation, do not produce significant amounts of DMS, but do form a disproportionately large part of the sinking flux of fixed carbon to the deep ocean. Modelling diatoms as a separate compartment is therefore tractable (because of their requirement for silicate) and will allow an improved representation of the biological pump and of DMS production. Iron is now recognised as an important micro-nutrient for phytoplankton, which can limit growth in some areas of the ocean (including the Southern Ocean and parts of the North and Equatorial Pacific). In many ocean areas iron found in the surface waters has mainly been supplied by atmospheric dust deposition (the Southern Ocean is an exception), and although utilisation by phytoplankton can be a temporary sink

this iron is quickly recycled and the long-term removal process is transfer to the sediments via adsorption onto mineral particles. Modelling iron cycling in the ocean allows us to examine possible climate feedbacks whereby increased dust production improves iron availability in the ocean, strengthening the biological pump and increasing the uptake of CO_2 by the ocean.

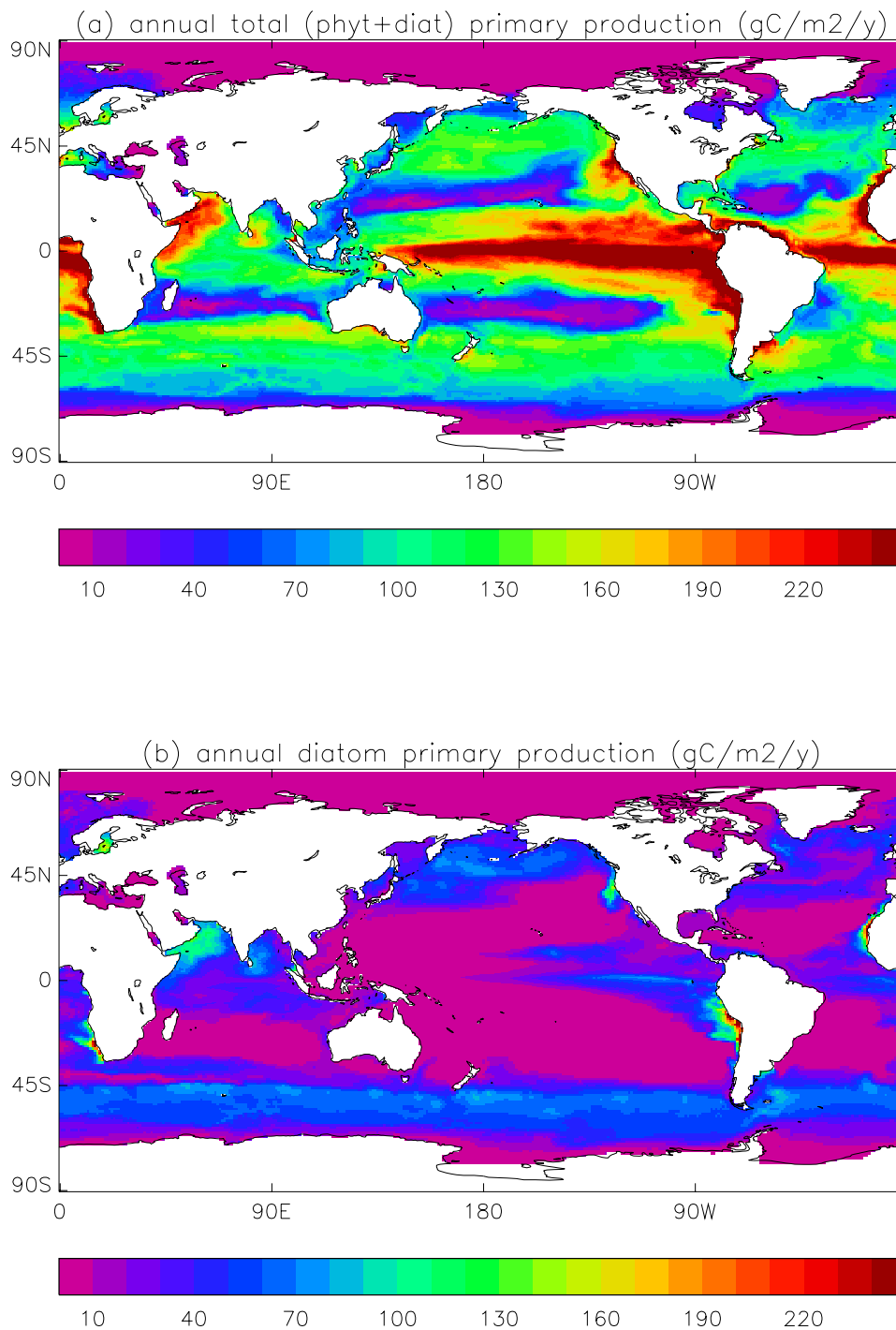


Figure 3.5: Annual mean primary production (fixation of carbon by photosynthesis) (a) by diatoms and other phytoplankton together, and (b) by diatoms alone

Each of the individual component parts of this biogeochemical system have been tested and shown to be technically correct. The complete model has also been analysed. In this configuration, the ocean biogeochemistry is coupled with the dynamic vegetation model and the interactive dust scheme. This means that iron input into the ocean from wind-borne dust is driven by the bare soil areas generated by the vegetation scheme. Figure 3.5 shows the annual mean primary production (fixation of carbon by photosynthesis) (a) by diatoms and other phytoplankton together, and (b) by diatoms alone. The totals are 42.8 and 8.8 GtC/y respectively, meaning that diatoms are responsible for 21% of the total primary production. Estimates of global annual productivity from remotely-sensed data range from below 40 to greater than 60 GtC/y (Carr et al. 2006). The original HadOCC model running in the same conditions has a global total of 53 GtC/y. So the Diat-HadOCC model has production that is within the estimated range, but near its lower bound. The difference between standard HadOCC and Diat-HadOCC production is mainly due to the additional limitation on growth due to iron. The North Pacific and Southern Ocean show iron limitation during their respective summers, the Equatorial Pacific is affected by iron limitation throughout the year and the North Atlantic is never iron-limited (because of high dust inputs from the Sahara). In contrast, the first three areas mentioned are never limited by the macro-nutrients (nitrate and silicate) in the model, but growth in the temperate North Atlantic shows seasonal macro-nutrient limitation. All these patterns of limitation are similar to those observed, giving confidence that the vegetation-dust-plankton coupled system can generate realistic productivity distributions. The global percentage of primary production that is due to diatoms, 21%, is below the estimate of 40% given by Tréguer et al. (1995); however the Tréguer figure includes coastal waters where diatom abundance is very high but which are mainly absent from the model. The pattern of total primary production is reasonable, with high seasonal production in the sub-polar regions and low production in the large sub-tropical gyres.

DMS is produced within Diat-HadOCC using the parameterisation of Simo and Dachs (2002). This scheme relates the DMS production to surface water chlorophyll concentrations and the depth of the corresponding mixed layer. The spatial distribution of model DMS production in most basins correlates well with that inferred from the standard DMS climatology (Kettle et al. 1999) (Figure 3.6(a) and (b)), however due to the small size of the dataset from which this climatology was produced, the climatology itself represents only a first order estimate of global ocean DMS values. To assess the relative ability of our model and the Kettle et al. climatology at capturing the spatial and temporal variability of DMS produced in the ocean, we have compared globally-averaged monthly DMS values from observations made since the Kettle et al. climatology was produced, with the corresponding predicted values at those sites from the model, and from the climatology (figure 3.6(c)). Detailed analyses are yet to be undertaken, but from this data it would appear that the modelled DMS values are equally, if not more, valid than those presented in the Kettle et al. climatology. It should be noted that these analyses have been made possible by the more than doubling in size of the DMS database since the Kettle et al. climatology was produced.

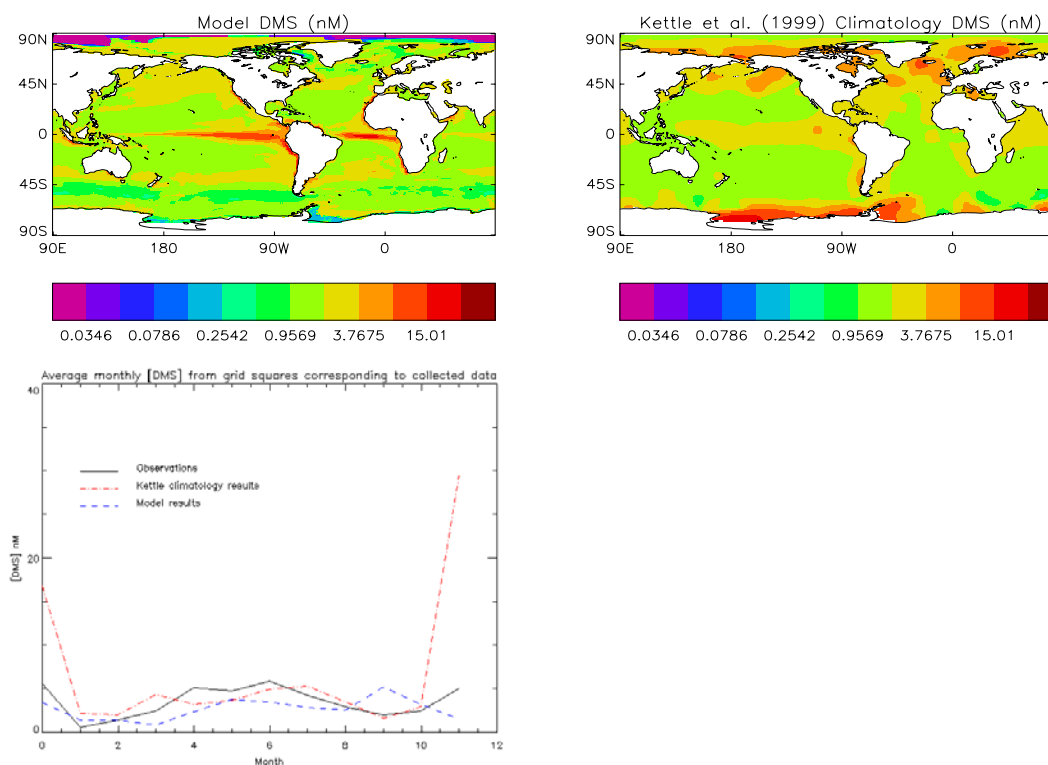


Figure 3.6 Surface ocean DMS concentrations a) Generated by HadGEM2 with the diat-HadOCC biology scheme b) from Kettle et al. (1999) climatology c) comparison of HadGEM2 and Kettle et al. against observations from <http://saga.pmel.noaa.gov/dms/>.

3.4 Evaluation of Chemistry Component of HadGEM2

3.4.1 Gas-phase chemistry

The atmospheric chemistry component of HadGEM2 is a configuration of the UKCA model (UK Chemistry and Aerosols www.ukca.ac.uk; O'Connor et al. in preparation) running tropospheric NO_x - HO_x - CH_4 - CO chemistry along with some representation of non-methane hydrocarbons. Large-scale transport (Davies et al., 2005), convective transport (Gregory and Rowntree 1990), and boundary layer mixing (Lock et al., 2000) of the 26 chemical tracers are included in the same manner as other model tracers. Bimolecular and termolecular reaction rate co-efficients make use of recommendations from the IUPAC (2005), JPL (2003), and the Master Chemical Mechanism vn3.1. Surface and aircraft emissions are prescribed as in O'Connor et al. (2004) and interactive lightning emissions of NO_x are included according to Price and Rind (1993). Photolysis rates are calculated offline in the Cambridge 2D model (Law and Pyle 1993) with the Hough (1988) scheme. Dry deposition is an adaptation of the Wesely (1989) scheme as implemented in the STOCHEM model (Sanderson et al., 2006). A complete suite of tracer and chemical diagnostics has also been included. Because the chemical scheme does not take account of halogen chemistry relevant to the stratosphere, stratospheric ozone concentrations are prescribed according to a climatology from Dall'Amico et al. 2008. These concentrations have lower values in the ozone maximum compared to those prescribed from SPARC (Randel and Wu 1999; Randel et al. 1999; Keihl et al. 1999) which are in the HadGEM2 version without interactive chemistry (as described in Stott et al. 2006).

The HadGEM2 with interactive chemistry has been run in an atmosphere-only configuration for 10 years. Figure 3.7 shows a comparison of the seasonal cycle of surface methane concentrations from the interactive run with climatological observations at 12 surface sites from the NOAA Global Monitoring Division network. It indicates that HadGEM2 is capable of representing both the seasonal cycle and absolute concentrations of surface methane very well. Statistical measures of skill have also been calculated. For example, the relative annual mean bias between the modelled and observed methane concentrations is better than 6 % at each of the surface sites.

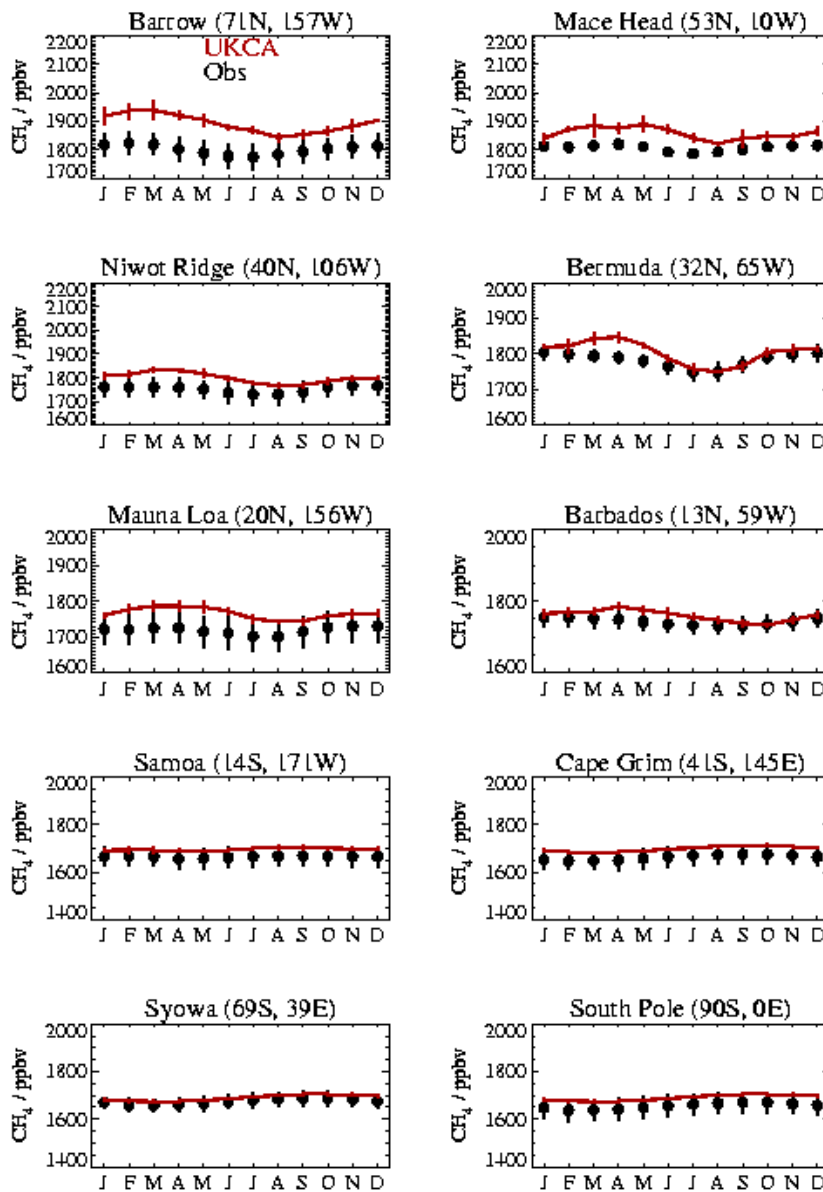


Figure 3.7: Comparison of modelled surface concentrations of methane from HadGEM2 interactive chemistry (red) with climatological observations (black) at 12 NOAA Global Monitoring Division surface.

Figure 3.8 shows comparisons of vertical ozone profiles in January from the HadGEM2 interactive chemistry run compared with non-interactive ozone and climatological observations at a subset of sites from Logan (1994). As above, the comparison indicates that the vertical ozone profiles from the run compares well with observations. It also suggests that the SPARC prescribed ozone concentrations are too low in the mid and lower troposphere, hence including interactive chemistry improves the representation of ozone.

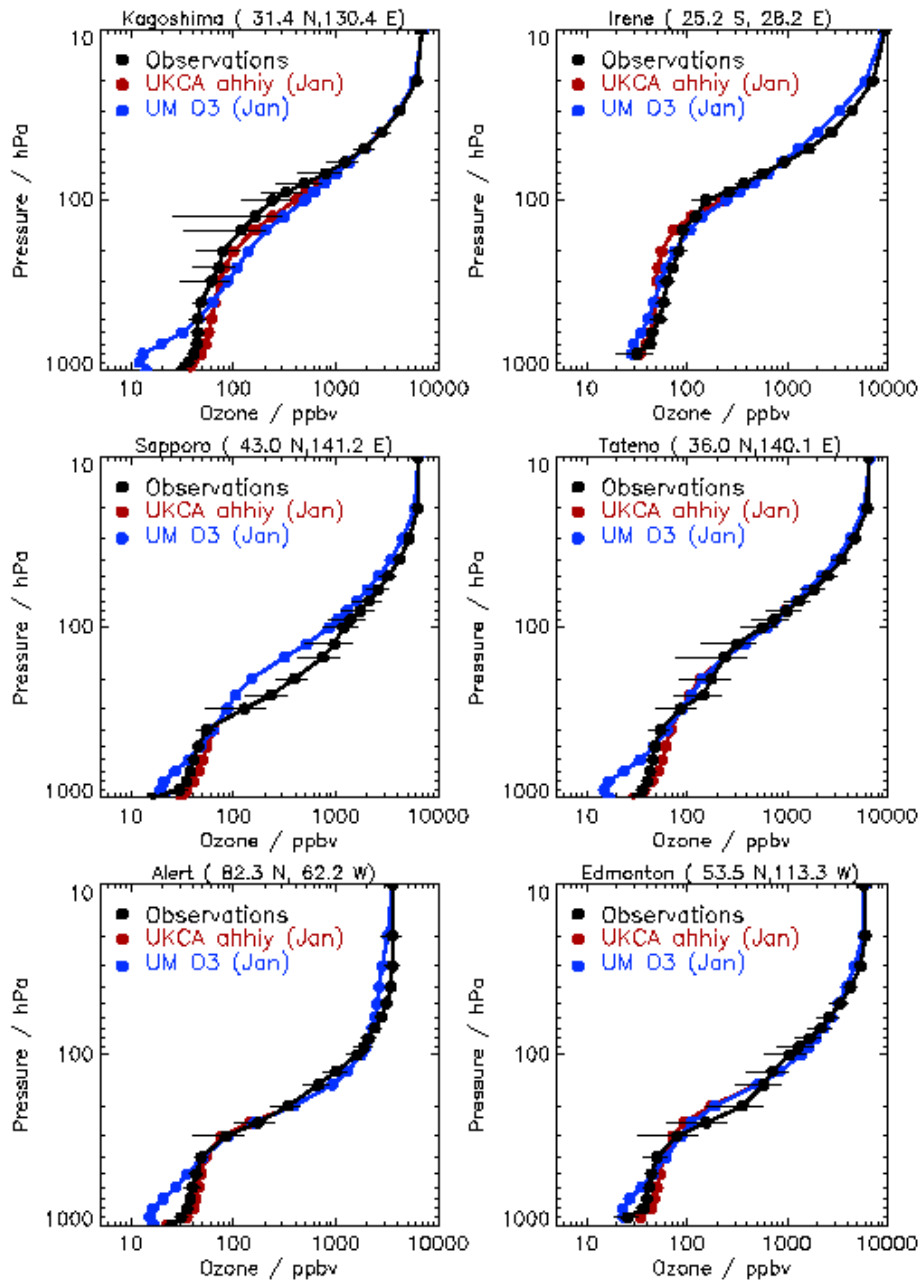


Figure 3.8: Comparison of modelled January vertical ozone profiles with climatological observations (black) from Logan (1994), interactive chemistry (red) and the prescribed ozone concentrations (blue).

A more quantitative assessment is plotted as a Taylor Diagram (Taylor 2001) in Figure 3.9, where interactively modelled and prescribed ozone concentrations are compared with the climatological observations at a number of different pressure levels using approximately 40 worldwide sites and all monthly output. In particular, it verifies that the global performance of modelled ozone from the UKCA interactive chemistry is much better than the prescribed ozone concentrations at pressure levels 300 hPa and below. At pressure levels 200 hPa and above, the comparison is effectively between the stratospheric climatologies of Dall’Amico et al., and SPARC. Although the overall global performance of interactively modelled ozone is better than the prescribed ozone, a closer inspection of modelled concentrations in the tropics indicates that the interactive ozone is higher than both the prescribed ozone and observations (not shown). This has implications for temperatures in the tropical tropopause region and is explored further in Section 4.1.

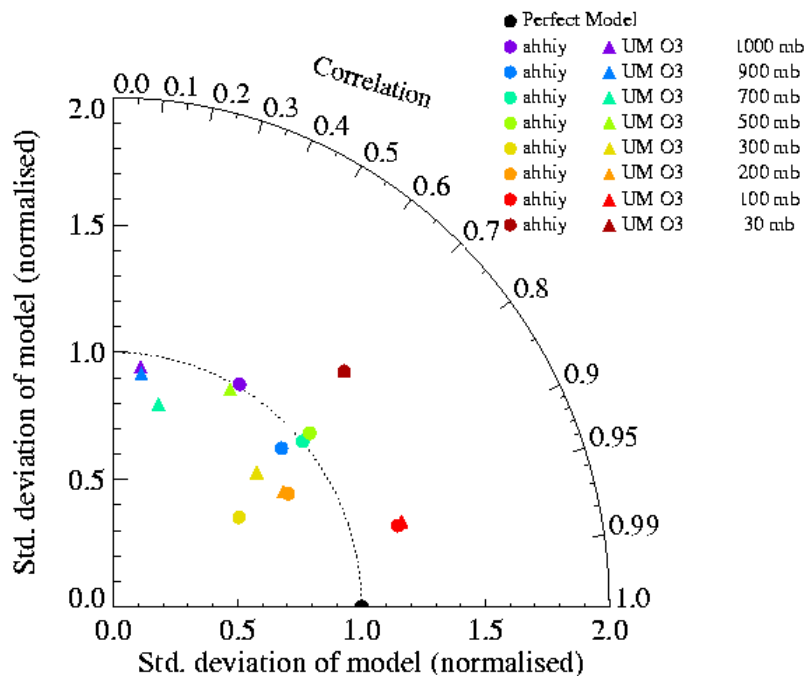


Figure 3.9: Taylor Diagram comparing modelled ozone with climatological observations from Logan (1994) at a number of pressure levels, using approximately 40 worldwide sites and all monthly output. The model data are from interactive chemistry (circles) and the non-interactive prescribed ozone (squares).

The UKCA interactive chemistry in HadGEM2 takes methane emissions from wetlands generated by the large-scale hydrology scheme (section 3.1) using the 4 soil carbon pools of Roth-C (section 3.2.2). The contributions from these pools are weighted such that pools with shorter lifetimes (hence decay more rapidly) have a higher weight. The overall scaling is chosen to give emissions of approximately 180 Tg methane per year. The emissions are shown in figure 3.10. As well as the major tropical wetlands, there are significant boreal emissions during the northern summer.

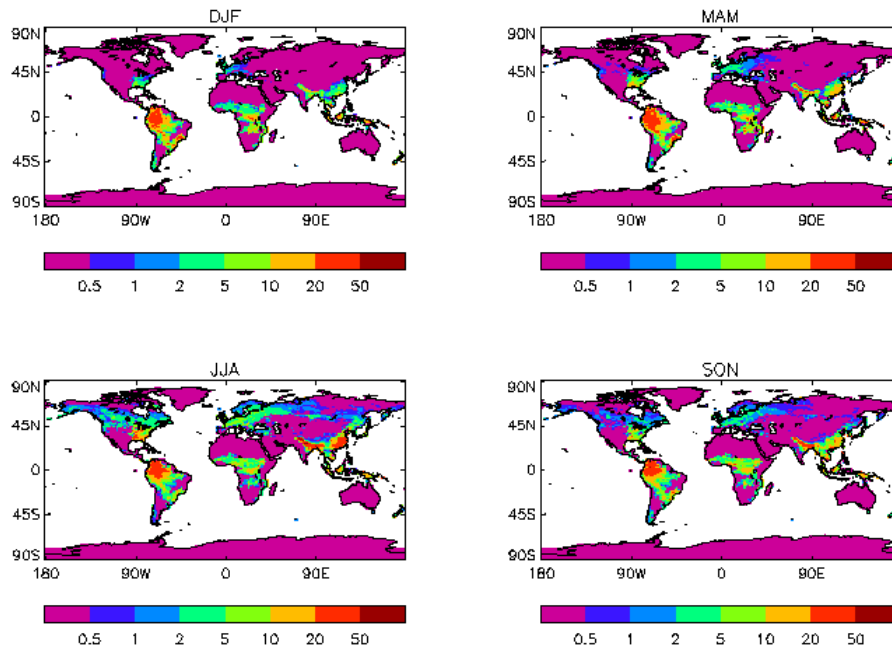


Figure 3.10: Distribution of emissions of methane from wetlands provided to UKCA by the large-scale hydrology scheme.

In summary, HadGEM2 performs well in global comparisons with both climatological surface observations and ozone vertical profiles. However, in the tropics, modelled ozone in the upper troposphere/lower stratosphere (UTLS) with the interactive chemistry is too high relative to both the non-interactive prescribed ozone and observations. This overestimate could have implications for tropical tropopause temperatures .

3.4.2 Updates to the sulphate aerosol chemistry

In the sulphur cycle in HadGEM2, DMS and SO₂ are oxidised by OH, H₂O₂, HO₂ and O₃. Previous versions of HadGEM have used concentrations of these oxidants obtained offline from the STOCHEM Chemistry Transport Model (see, e.g., Collins *et al.*, 1997), and supplied to HadGEM as prescribed monthly mean fields which do not vary with changing emissions and climate. Rae *et al.* (2007) studied the effects on sulphate aerosol in HadGEM1 of changing the input oxidant concentrations from present-day values to values consistent with late-21st century predictions of emissions and climate. They found that changing the oxidants alone led to changes in sulphate aerosol burden of a comparable magnitude to the changes induced by changing the climate boundary conditions and greenhouse-gas concentrations, and concluded that it is important to represent, in a climate model, oxidant changes due to changes in emissions and climate. To do this requires the introduction of coupling between climate, chemistry and aerosols, which has now been done in HadGEM2 by coupling the HadGEM sulphur scheme to the UKCA tropospheric chemistry scheme. Modelled sulphate concentrations obtained with online oxidants have been found to compare with observations at least as favourably as those obtained with prescribed oxidants. In addition, the introduction of this coupling will permit investigations of climate-chemistry-aerosol feedbacks.

3.5 Dust coupled to the earth system components

In the earth system configuration, the HadGEM2 mineral dust scheme uses the bare soil fraction generated by the dynamic vegetation scheme. It has been assessed using results from 10 years of an atmosphere-only simulation, following 13 years dynamic spin-up of the vegetation. The results were rather different from those generated using climatological bare soil distributions. Global dust production was more than twice as high, and the atmospheric load was also correspondingly higher (figure 3.11). The extra dust emissions were mainly generated in Australia, India, North Africa and the Middle East and were predominantly caused by increases in bare soil source areas due to loss of vegetation, simulated by the dynamic vegetation scheme. A secondary effect of vegetation loss was an increase in low-level windspeeds, which also enhanced dust production. The excessively high dust load was also evident in comparisons with observations of near-surface concentrations and optical depths (figure 3.12).

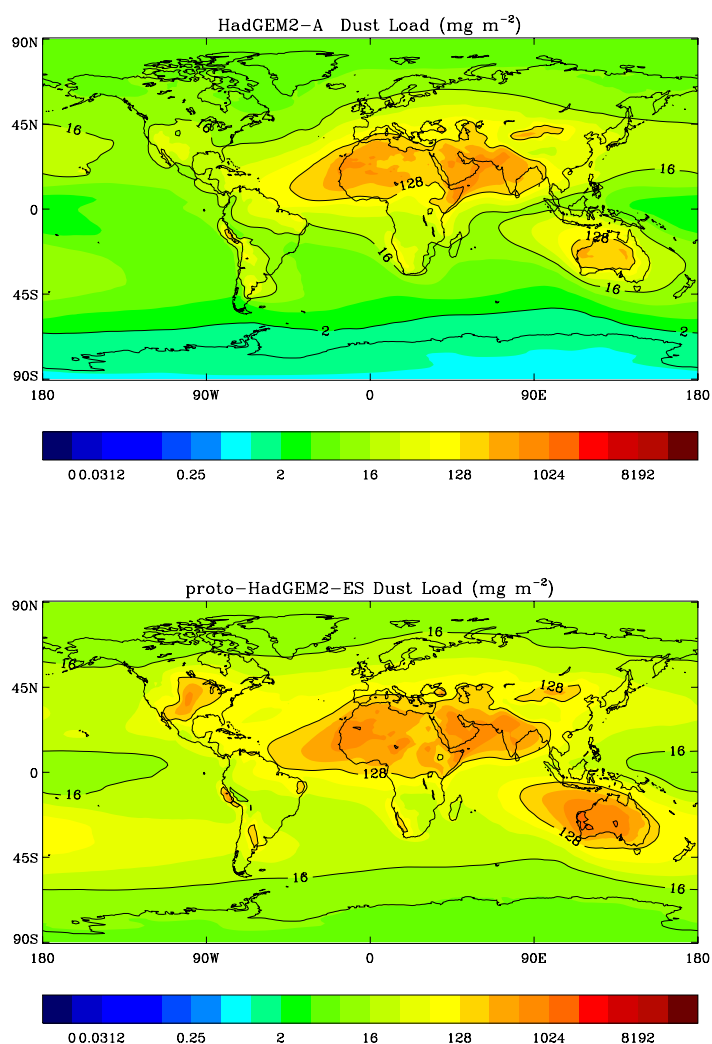


Figure 3.11. Decadal mean dust load (mg m^{-2}) from climatological vegetation (above) and dynamic vegetation (below).

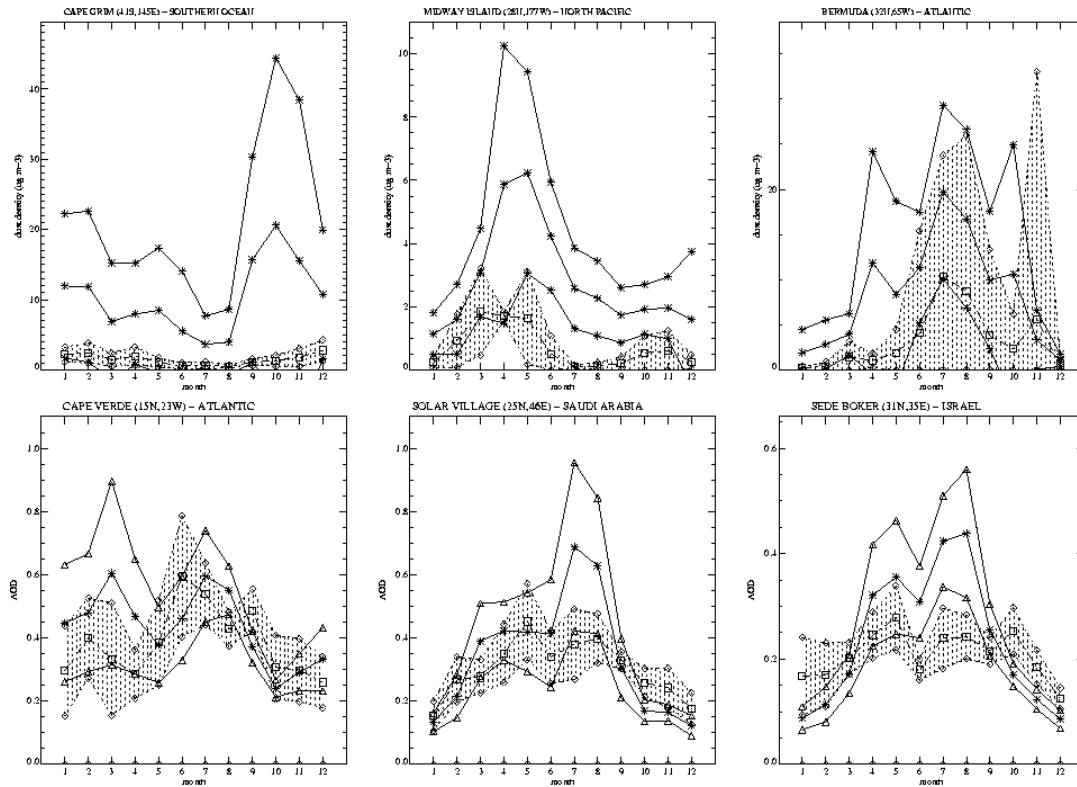


Figure 3.12 Comparison of HadGEM2 with interactive vegetation and observed annual cycles of mineral dust fields. Note these results compare directly with those shown in figure 2.13.

The coupling together of various interactive schemes, as in this case, will inevitably lead to changes in the model simulation. The dust fields are not expected to be as close to reality as in the more constrained situation. Whether the very large dust fields with interactive vegetation are acceptable will depend on the application.

3.6 Carbon Cycle simulations

In this section we assess the behaviour of the carbon cycle in HadGEM2, with the atmospheric CO₂ concentrations determined by the carbon fluxes from the terrestrial and ocean ecosystem components. The seasonal cycle in the model is particularly dependent on the balance between the NPP and the soil respiration. The improvements to the terrestrial carbon fluxes described in section 3.1.3 give very good agreement between the simulated and observed atmospheric CO₂ concentrations. As shown in figure 3.13, the seasonal cycle is much better in HadGEM2 compared to HadCM3.

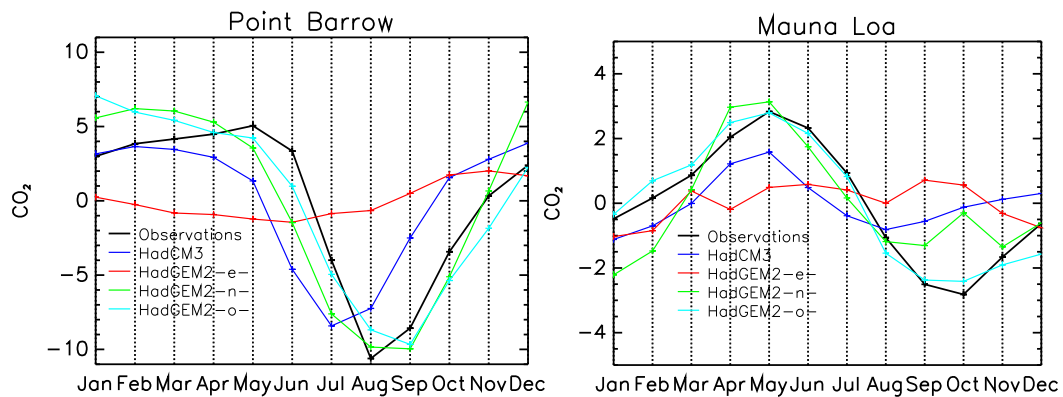


Figure 3.13. Observed (Keeling et al. 2008) and simulated seasonal cycles of atmospheric CO₂ (in ppm) comparing final HadGEM2 tuning (turquoise) and HadCM3 (blue).

4 Evaluation of the physical climate with the earth system components coupled

The physical climate of HadGEM without the earth system components has been evaluated and found to perform well in section 2. However we want to interactively simulate earth system components rather than specifying them from observed climatologies. This will allow us to understand how feedbacks in the earth system may affect our predictions of future climate change. Introducing interactive components rather than using climatologies inevitably degrades the overall simulation of the present day climate since no interactive scheme is perfect. However we expect our simulation of future climate to be better using an earth system model. The two earth system components having the largest effect on the simulation of the present physical climate are the vegetation scheme and the chemistry scheme. In this section we quantify their impact on the ability to simulate present climate.

4.1 Effect of large-scale hydrology

The general increase in soil moisture due to the LSH scheme tends to cool the surface temperatures. This can be seen in figure 4.1 for an AMIP run which shows a cooling of the 1.5m temperature especially in Siberia and Canada, leading generally to an improvement in the comparison with the climatology in these regions. However this has made the far north east of Russia, and Alaska and the far north west of Canada too cold. Globally the LSH scheme decreases the TOA radiation balance by 0.2 Wm^{-2} in the AMIP run.

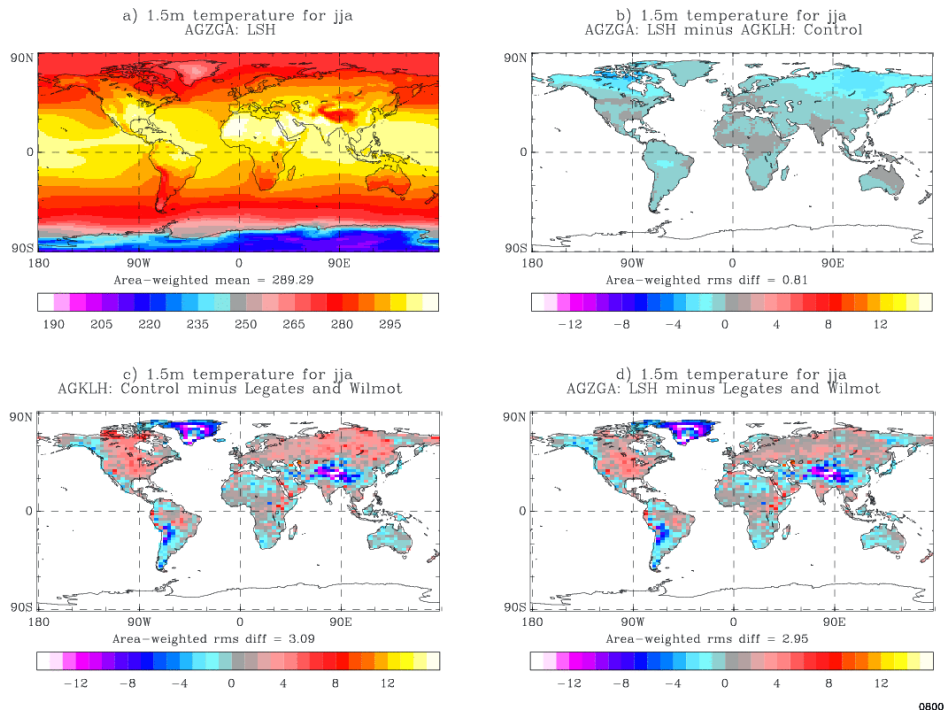


Figure 4.2. Northern summer (JJA) surface air temperature at 1.5m from HadGEM2 with LSH, AMIP simulation (top left); difference due to LSH (top right) and differences from Legates and Wilmot climatology without and with LSH (left and right bottom panels).

4.2 Effect of dynamic vegetation.

The vegetation cover simulated by TRIFFID in HadGEM2 is generally good, but has some deficiencies as described in section 3.2. In particular a lack of vegetation in north and east Siberia where the model simulates too much bare soil, and a lack of vegetation in both India and Australia where the model also simulates too much bare soil. The model also tends to simulate too strong southward extent of tropical forest into savannah areas probably due to lack of anthropogenic or fire disturbance.

These features have implications for other earth system components, especially the emission of dust from the land surface as discussed in section 3.5. In this section we assess their implications for the simulation of physical climate. We perform an AMIP simulation for the period 1978 to 2003 and validate the model performance of HadGEM2 against a version with fixed vegetation distribution. Both versions included the large-scale hydrology scheme.

Overall we find no significant differences between the two simulations. The net downward radiation at the top of the atmosphere decreased slightly from 1.11 Wm^{-2} to 1.08 Wm^{-2} . The simulation with simulated land cover shows generally reduced land surface temperatures in Northern summer (Figure 4.2) which act to improve validation against observations in many places. Slight reduction in precipitation over boreal land areas and slightly wetter tropical land areas also improves the validation slightly (Figure 4.3).

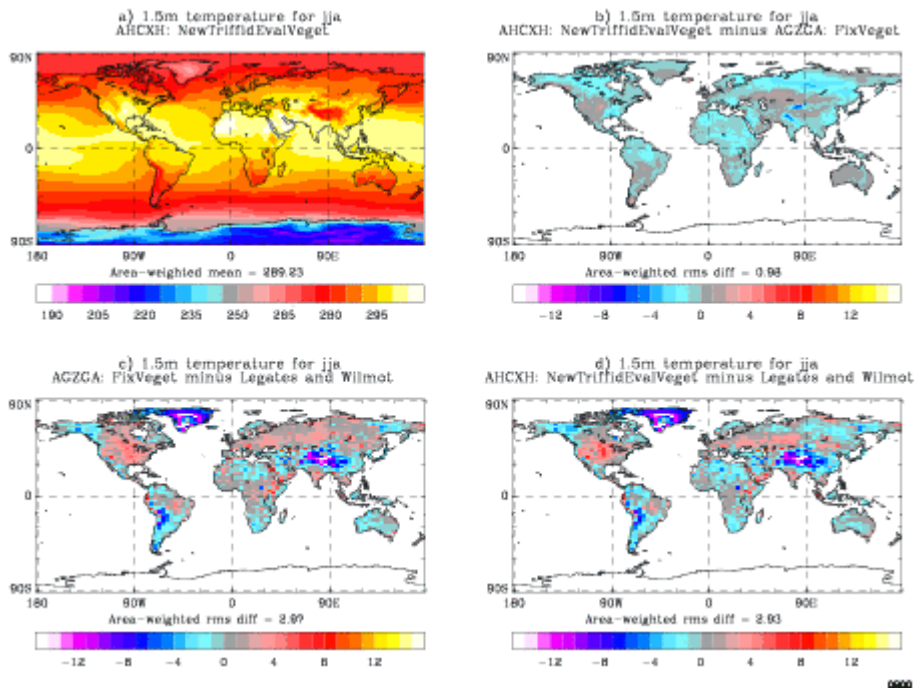


Figure 4.2. Northern summer (JJA) surface air temperature at 1.5m from HadGEM2 with dynamic vegetation AMIP simulation (top left); difference due to adding dynamic vegetation (top right) and differences from Legates and Wilmot climatology without and with dynamic vegetation (left and right bottom panels).

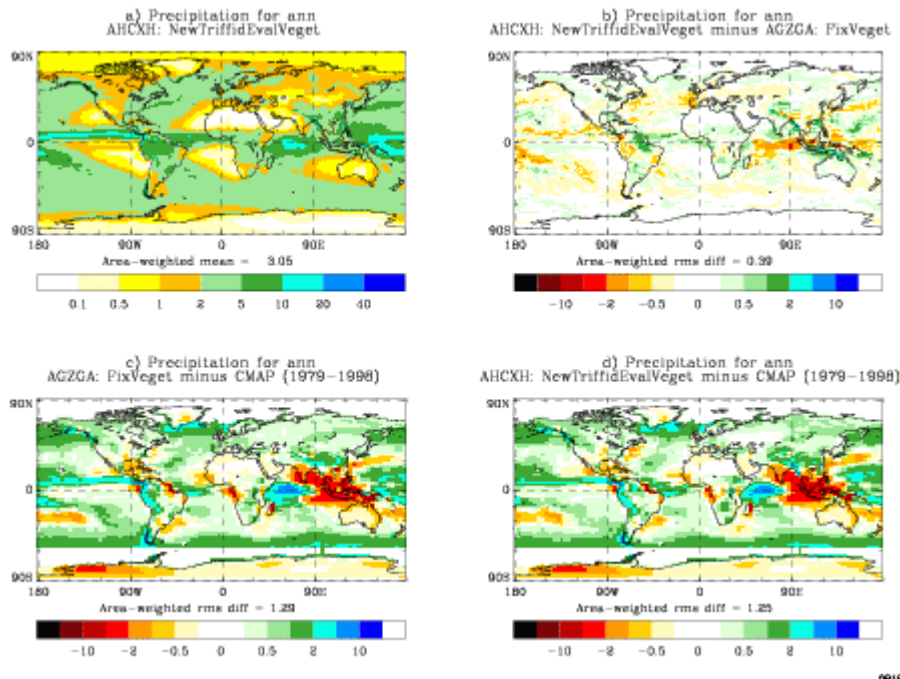


Figure 4.3 Annual mean precipitation from HadGEM2 AMIP simulation with dynamic vegetation (top left); difference due to adding dynamic vegetation (top right) and differences from CMAP climatology without and with dynamic vegetation (left and right bottom panels).

The simulated excess of bare ground over Siberia results in altered surface fluxes of latent and sensible heat. Top level (0-10cm) soil moisture is drier with dynamic vegetation as a result of reduced precipitation. Lower level soil moisture (35-100cm) is wetter as a result of less tapping of roots into the deep stored soil moisture. Albedo is also affected over north east Asia in winter with much brighter land surface in the

dynamic vegetation simulation because snow covered bare ground has greater albedo than snow covered trees. However, the impact of albedo and surface heat flux changes over Siberia do not seem to have a significant effect on the large scale circulation or surface climate variables, and we conclude that the model simulation of physical climate is not significantly degraded by the inclusion of an dynamic vegetation scheme.

4.3 Effect of interactive chemistry on mean climate

Ozone absorbs both solar and infrared radiation and, in particular, the radiative forcing efficiency on a per molecule basis is greatest for ozone changes near the tropopause (Lacis et al., 1990). As a result, any difference between HadGEM2 UKCA interactive and prescribed ozone concentrations has the potential to alter the mean climate. In addition, with prescribed ozone HadGEM2 makes use of a scheme from HadGEM1 (Martin et al., 2006), called “tropopause matching”, in which the ozone distribution was vertically re-distributed to take into account changes in the tropopause position. However, with interactive chemistry, tropopause matching is no longer required as the ozone and tropopause location will inherently be consistent. Since methane is well-mixed compared to ozone, differences between the interactive and non-interactive methane distributions for present day conditions are likely to have a very small impact on the radiation.

Figure 4.4 shows the zonal mean temperatures for the Dec-Jan-Feb (DJF) time period from 10 year AMIP atmosphere-only integrations with and without interactive ozone and methane fields. It indicates that the tropical tropopause temperatures are higher compared to prescribed ozone by approximately 1K. HadGEM2 already had a warm bias in that region relative to ECMWF re-analyses which has been made worse by the inclusion of interactive ozone and/or by switching off tropopause matching. Although the tropical tropopause temperature bias with ECMWF re-analyses has increased to 2K in DJF and in JJA (not shown), it is still within the spread of tropical tropopause temperature biases seen in an evaluation of 13 coupled chemistry-climate models by Eyring et al. (2006).

A separate integration with prescribed ozone, but without tropopause matching indicates that tropopause matching does not contribute to the change in tropical tropopause temperatures. The change in tropical tropopause temperatures can be solely attributed to the inclusion of interactive ozone and is consistent with zonal mean differences between interactive and prescribed ozone concentrations. In terms of radiation fluxes, the global annual net downward radiation flux at the top of the atmosphere (TOA) increased from 1.03 Wm^{-2} to 1.44 Wm^{-2} with interactive chemistry. Half of the increase can be attributed to switching off tropopause matching and the remainder is due to the inclusion of radiative feedback from interactive ozone and methane.

In summary, the mean climate for the present day differs due to switching off tropopause matching and switching on UKCA interactive chemistry. Although both equally contribute to the change in the TOA global annual net downward radiation flux, it is the switch from prescribed to interactive ozone that is responsible for the increase in the bias of tropical tropopause temperatures. Simulations for 1860 show

similar impacts of interactive chemistry on the temperatures, but the impact on the TOA balance is much less ($+0.1 \text{ Wm}^{-2}$).

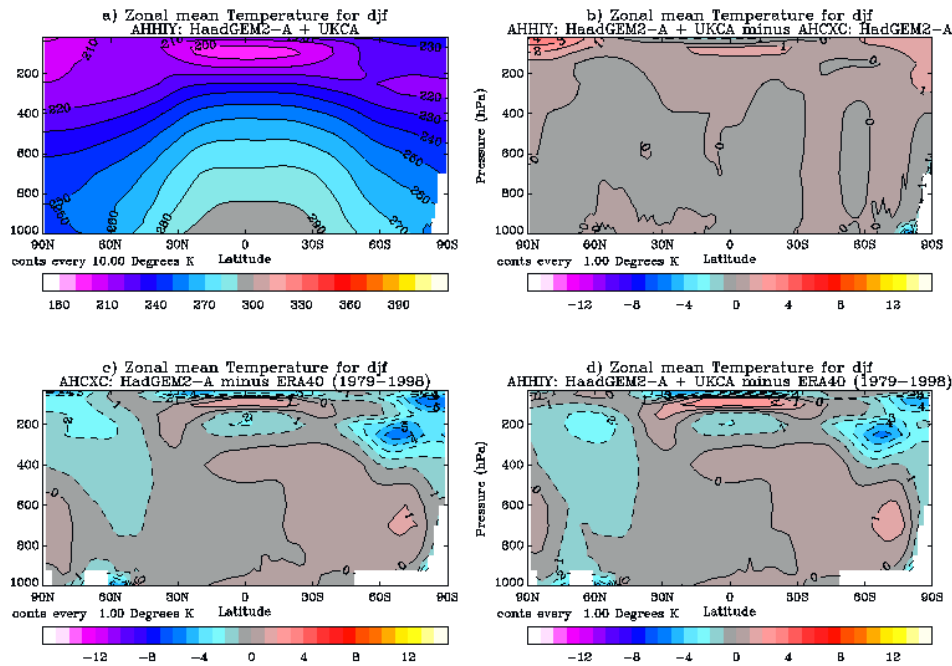


Figure 4.4: a) Zonal mean temperatures for the Dec-Jan-Feb (DJF) time period with interactive ozone and methane fields; b) Difference in DJF zonal mean temperatures between interactive and prescribed chemistry; c) Difference in DJF zonal mean temperature with prescribed chemistry and ECMWF re-analyses; and d) Difference in DJF zonal mean temperature with interactive chemistry and ECMWF re-analyses.

4.3 Effect of ocean biology on radiative balance

As well as affecting the atmospheric CO_2 levels, the ocean biology affects the climate through the DMS emissions (section 3.3). These lead to sulphate aerosol, which in turn can affect cloud properties. Figure 4.5 shows the difference in short wave cloud forcing between two atmosphere-only runs; one using the standard Kettle et al. (1999) DMS database, the other using monthly-mean DMS concentrations from the full HadGEM2 model (figure 3.6). The overall change in top-of-atmosphere balance is $+0.21 \text{ Wm}^{-2}$ after adding in the modelled DMS. As can be seen in figure 4.5, this is due to less outgoing short wave radiation (positive forcing) in the Southern Ocean as there are lower DMS emissions here in the model compared to the climatology.

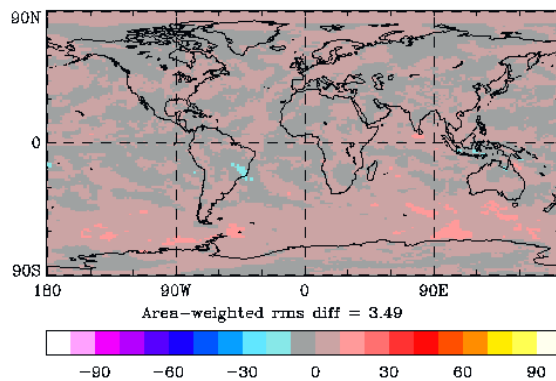


Figure 4.6: Change in cloud forcing (Wm^{-2}) due to using the modelled DMS distributions rather than the Kettle database.

5 Outstanding issues

After the simulations for this note were performed a bug was discovered in the Rayleigh scattering code. This is not expected to affect any of the discussions or conclusions presented here, but does mean that the HadGEM2 model will need to be re-tuned to achieve TOA radiation balance. The configurations of HadGEM2 with and without the earth system components differ by around 0.1 Wm^{-2} so it is hoped that the re-tuning will be equally applicable for both configurations.

A small bug overestimating the evaporation from arid soils has been found. Fixing this is likely to give a slight increase in soil moisture in arid areas, but to have little overall effect on model performance.

References

- Anderson, T. R., S. A. Spall, A. Yool, P. Cipollini, P. G. Challenor, and M. J. R. Fasham, 2001., Global fields of sea surface dimethylsulphide predicted from chlorophyll, nutrients and light, *J. Mar. Res.*, 30, 1–20
- Bagnold, R.A., 1941, *The Physics of Blown Sand and Desert Dunes*, Methuen, New York
- Banks et al, 2008. Evaluation of HadGEM3-AO. ICP deliverable Q2
- Bellouin, N., *et al.*, Improved representation of aerosols for HadGEM2, Hadley Centre Technical Note No. 73, 2007, 42pp.
- Betts, R.A., Falloon, P.D., Klein Goldewijk K. and Ramankutty N., 2007. Biogeophysical effects of land use on climate: model simulations of radiative forcings and large-scale temperature change. *Agric. Forest Meteorol.* **142** 216-233 doi:0.1016/j.agrformet.2006.08.021
- Beven, K. J., and M. J. Kirkby, 1979, A physically based, variable contributing area model of basin hydrology, *Hydrol. Sci. Bull.*, 24, 43–69.
- Bond, T. C., E. Bhardwaj, R. Dong, R. Jogani, S. Jung, C. Roden, D. G. Streets, and N. M. Trautmann, 2007., Historical emissions of black and organic carbon aerosol from energy-related combustion, 1850–2000, *Global Biogeochem. Cycles*, 21, GB2018, doi:10.1029/2006GB002840.
- Brown AR, and Grant AL, 1997. Non-local mixing of momentum in the convective boundary layer. *Boundary-Layer Meteorol.*, 84, 1-22.
- Carr, M.-E. et al., 2006. A comparison of global estimates of marine primary production from ocean color, *Deep Sea Research Part II: Topical Studies in Oceanography* Volume 53, Issues 5-7, Pages 741-770.
- Clark DB and Gedney N. 2008. Representing the effects of subgrid variability of soil moisture on runoff generation in a land surface model *J. Geophys. res.* **113** D10111, doi:10.1029/2007JD008940
- Coleman, K. and Jenkinson, D. S. 1999, RothC-26.3, A model for the turnover of carbon in soil: Model description and User's guide Lawes Agricultural Trust Harpenden, UK
- Collins, W.J., D.S. Stevenson, C.E. Johnson and R.G. Derwent ,1997. Tropospheric ozone in a global-scale three-dimensional model and its response to NO_x emission controls. *J. Atmos. Chem.*, **26**, 223—274.
- Cox, P.M. 2001. Description of the TRIFFID Dynamic Global Vegetation Model Hadley Centre, Met Office, Technical Note 24.

- Cox, P.M., R.A. Betts, C.D. Jones, S.A. Spall, I.J. Totterdell. 2000, Acceleration of global warming due to carbon-cycle feedbacks in a coupled climate model. *Nature* **408**, 184 - 187 , doi: 10.1038/35041539
- Cox PM, R. A. Betts and C. B. Bunton and R. L. H. Essery and P. R. Rowntree and J. Smith, 1999. The impact of new land surface physics on the GCM simulation of climate and climate sensitivity *Clim. Dyn.* 15 183-203
- Cramer, W., D. W. Kicklighter, A. Bondeau, B. Moore III, G. Churkina, B. Nemry, A. Ruimy, A. L. Schloss and The Participants of the Potsdam NPP Model Intercomparison, 1999. Comparing global models of terrestrial net primary productivity (NPP): overview and key results. *Global Change Biology*, Volume 5 Issue S1:1-15
- Dall'Amico, M., L.J. Gray, K.H. Rosenlof, A.A. Scaife and P.A. Stott. 2008, Climate model simulations of recent decades with improved stratospheric representation: variability and trends in the stratosphere. Submitted to *Clim. Dyn.*
- T. Davies, M. J. P. Cullen, A. J. Malcolm, M. H. Mawson, A. Staniforth, A. A. White, and N. Wood, 2005. A new dynamical core for the Met Office's global and regional modelling of the atmosphere, *Q. J. Roy. Meteorol. Soc.*, 131, 608, 1759-1782,
- Davidson E. and Janssens I, 2006. Temperature sensitivity of soil carbon decomposition and feedbacks to climate change. *Nature.*, 440: 165-173
- Davison, P.S., Roberts, D.L., Arnold, R.T., and Colvile, R.M., 2004. Estimating the direct radiative forcing due to haze from the 1997 forest fires in Indonesia. *J. Geophys. Res.*, 109, doi:10.1029/2003JD00424.
- Debell L.J. et al. 2006. Spatial and Seasonal Patterns and Temporal Variability of Haze and its Constituents in the United States: Report IV. CIRA Colorado State University
- Dentener, F. et al., 2006. Emissions of primary aerosol and precursor gases in the years 2000 and 1750, prescribed data-sets for AeroCom. *Atmos. Chem. Phys.*, 6, 4321-4344.
- Essery, R. L. H., M. J. Best, R. A. Betts, P. M. Cox, and C. M. Taylor, 2003. Explicit representation of subgrid heterogeneity in a GCM land surface scheme, *J. Hydrometeorol.*, 4, 530–543.
- V. Eyring, N. Butchart, D.W. Waugh, H. Akiyoshi, et al., 2006. Assessment of temperature, trace species, and ozone in chemistry-climate model simulations of the recent past, *J. Geophys. Res.*, 111, D22308, doi:10.1029/2006JD007327.
- Fecan F. et al., 1999. Parameterisation of the increase of the Aeolian erosion threshold wind friction velocity due to soil moisture for arid and semi-arid areas. *Ann. Geophys.* 17, 149-157.
- Friedlingstein et al., 2006, Climate-carbon cycle feedback analysis, results from the C4MIP model intercomparison. *J. Climate* **19**(14) 3337-3353 doi:10.1175/JCLI3800.1.
- Gedney N and P.M. Cox, 2003. The sensitivity of global climate model simulations to the representation of soil moisture heterogeneity *J. Hydrometeorology* **4** (6) 1265-1275
- Gedney, N., P. M. Cox, and C. Huntingford, 2004. Climate feedback from wetland methane emissions, *Geophys. Res. Lett.*, 31, L20503, doi:10.1029/2004GL020919.
- D. Gregory and P.R. Rowntree, 1990. A mass flux convection scheme with representation of cloud ensemble characteristics and stability-dependent closure, *Mon. Wea. Rev.*, 118, 1483-1506.
- Gunson, J. R., S. A. Spall, T. R. Anderson, A. Jones, I. J. Totterdell, and M. J. Woodage, 2006. Climate sensitivity to ocean dimethylsulphide emissions, *Geophys. Res. Lett.*, 33, L07701, doi:10.1029/2005GL024982

Haywood, J.M. et al., 2003. The mean physical and optical properties of regional haze dominated by biomass-burning aerosol measured from the C-130 aircraft during SAFARI 2000. *J. Geophys. Res.*, **108**, doi:10.1029/2002JD002226.

Hjellbrekke, A.-G., 2002, Data report 2000 Acidifying and eutrophying compounds. Part1: Annual summaries – EMEP/CCC-Report 6/2002, Norwegian Institute for Air Research, PO Box 100, NO-2027, Kjeller, Norway.

A. M. Hough, 1998. The calculation of photolysis rates for use in global tropospheric modelling studies, At. Energy Res. Estab. Report, 13259, Harwell, UK,.

IUPAC Subcommittee for Gas Kinetic Data Evaluation, March 2005. Summary of evaluated kinetic data and photochemical data for atmospheric chemistry, (plus data sheets), All at: <http://www.iupac-kinetic.ch.cam.ac.uk/>

T.C. Johns, C.F. Durman, H.T. Banks, M.J. Roberts, A.J. McLaren, J.K. Ridley, C.A. Senior, K.D. Williams, A. Jones, G.J. Rickard, S. Cusack, W.J. Ingram, M. Crucifix, D.M.H. Sexton, M.M. Joshi, B-W. Dong, H. Spencer, R.S.R. Hill, J.M. Gregory, A.B. Keen, A.K. Pardaens, J.A. Lowe, A. Bodas-Salcedo, S. Stark, and Y. Searl, 2006. The new Hadley Centre climate model HadGEM1: Evaluation of coupled simulations. *Journal of Climate*, 19, 1327-1353.

Jones A., D.L. Roberts, M.J. Woodage, and C.E. Johnson, 2001. Indirect sulphate aerosol forcing in a climate model with an interactive sulphur cycle. *J. Geophys. Res.*, *106*, D17, 20293—29310.

Jones CD, McConnell C, Coleman KW, Cox P, Falloon PD, Jenkinson D, Powlson D, 2005. Global climate change and soil carbon stocks; predictions from two contrasting models for the turnover of organic carbon in soil. *Global Change Biol.* 11: 154-166, doi: 10.1111/j.1365-2486.2004.00885.x.

Jones, C.D., Doutriaux-Boucher, M., Liddicoat, S., Sitch, S. 2008. Simulation of the Terrestrial Carbon Cycle by HadGEM2-ES. Internal Met Office HadGEM2 report, March 2008.

JPL, Chemical Kinetics and Photochemical Data for Use in Atmospheric Studies. , February 2003. Evaluation Number 14, JPL Publication 02-25.

Keeling, R.F., S.C. Piper, A.F. Bollenbacher and J.S. Walker. 2008. Atmospheric CO₂ records from sites in the SIO air sampling network. In Trends: A Compendium of Data on Global Change. Carbon Dioxide Information Analysis Center, Oak Ridge National Laboratory, U.S. Department of Energy, Oak Ridge, Tenn., U.S.A

Kiehl, J.T., T.L. Schneider, R.W. Poltmann, and S. Solomon, 1999, Climate forcing due to tropospheric and stratospheric ozone. *J. Geophys. Res.*, **104**, 31239-31254

Kettle, A. J., et al., 1999. A global database of sea surface dimethylsulfide (DMS) measurements and a procedure to predict sea surface DMS as a function of latitude, longitude, and month, *Global Biogeochem. Cycles*, 13, 399–444

Klein Goldewijk K., 2001. Estimating global land use change over the past 300 years: The HYDE Database *Global Biogeochem. Cycles* **15** (2) 417-433.

A.A. Lacis, D.J. Wuebbles, and J.A. Logan, 1990. Radiative Forcing of Climate by Changes in the Vertical Distribution of Ozone, *J. Geophys. Res.*, *95*, D7, 9971-9981.

K.S. Law and J.A. Pyle, 1993. Modelling Trace Gas Budgets in the Troposphere .1. Ozone and Odd Nitrogen, *J. Geophys. Res.*, *98*, 18377-18400.

A. P. Lock, A. R. Brown, M.R. Bush, G.M. Martin, and R.N.B. Smith, 2000. A new boundary layer mixing scheme. Part I: Scheme description and single-column model tests, *Mon. Wea. Rev.*, *128*, 3187-3199.

- J.A. Logan, 1994. Trends in the vertical-distribution of ozone - an analysis of ozonesonde data, *J. Geophys. Res.*, 99, D12, 25553-25585.
- Maidens, AV and Derbyshire SH, 2006. Improving mass flux profiles in the Gregory-Rowntree convection scheme using adaptive detrainment. *Q. J. R. Meteorol. Soc.*, 128. doi:10.1256/qj.2006.n
- Martcorena B. and G. Bergametti, 1995, Modeling the atmospheric dust cycle, 1,1 Design of a soil-derived dust emission scheme, *J. Geophys. Res.* 100, 16,415-16,450.
- Martin, GM et al.. Analysis and reduction of climate model systematic errors through a unified modelling strategy. In preparation.
- G. M. Martin, M.A. Ringer, V.D. Pope, A. Jones, C. Dearden, and T.J. Hinton, 2006. The Physical Properties of the Atmosphere in the New Hadley Centre Global Environmental Model (HadGEM1). Part 1: Model Description and Global Climatology, *J. Climate*, 19, 1274-1301.
- Master Chemical Mechanism v3.1,
<http://www.chem.leeds.ac.uk/Atmospheric/MCM/mcmproj.html>
- Mercado, L. M., Huntingford, C., Gash, J. H. C., Cox, P. M., and Jogireddy, V., 2007. Improving the representation of radiation interception and photosynthesis for climate model applications, *Tellus*, 59B, 553–565.
- Moum JN and Osbourne TR, 1986. Mixing in the main thermocline. *J. Phys. Oceanography*, 16, 1250-1259.
- Murphy, et al, 2004. Quantification of modelling uncertainties in a large ensemble of climate change simulations. *Nature*, 430, 768-772.
- National Oceanic & Atmospheric Administration , Global Monitoring Division,
<http://www.esrl.noaa.gov/gmd/>
- F.M. O'Connor et al. Evaluation of the new UKCA climate-composition model. Part 2: The troposphere. In preparation
- F.M. O'Connor, K.S. Law, J.A. Pyle, H. Barjat, N. Brough, K. Dewey, T. Green, J. Kent, and G. Phillips, 2004. Tropospheric Ozone Budget: Regional and Global Calculations, *Atmos. Chem. Phys. Discuss.*, 4, 991-1036.
- Palmer, J. R., and I. J. Totterdell, 2001. Production and export in a global ocean ecosystem model, *Deep Sea Res.*, Part I, 48, 1169–1198
- C. Price and D. Rind, 1993. What determines the cloud-to-ground lightning fraction in thunderstorms?, *Geophys. Res. Letts.*, 20, 6, 463-466.
- Rae J.G.L. 2008. Sulphate aerosol in a climate model: effect of using on-line oxidants. MSc dissertation, University of Reading.
- Rae J.G.L., C.E. Johnson, N. Bellouin, O. Boucher, J.M. Haywood and A. Jones, 2007. Sensitivity of global sulphate aerosol production to changes in oxidant concentrations and climate. *J. Geophys. Res.*, 112, D10312, doi:10.1029/2006JD007826.
- Randel, W.J. and F. Wu, 1999, A stratospheric ozone trends dataset for global modelling. *Geophys. Res. Lett.*, 26, 3089-3092.
- Randel, W.J., R. Stolarski, D. M. Cunnold, J. A. Logan, M.J. Newchurch and J.M. Zawodny, 2003, Atmosphere-trends in the vertical distribution of ozone. *Science*, 285, 1689-1692

Reddy, M.S., O. Boucher, Y. Balkanski and M. Schulz, 2005. Aerosol optical depth and radiative forcing by species and source types in the LMDZT General Circulation Model, *Geophys. Res. Lett.*, 32 (L12803), doi:10.1029/2004GL021743.

Reichler, T, and Kim J, 2008. How well do coupled models simulate today's climate? *Bull. American Met. Soc* **89**, 303–311.

M.G. Sanderson, W.J. Collins, C.E. Johnson, and R.G. Derwent, 2006. Present and future acid deposition to ecosystems: The effect of climate change, *Atmos. Environ.*, 40, 1275-1283.

Simo R, Dachs J., 2002, Global ocean emission of dimethylsulfide predicted from biogeophysical data. *Global Biogeochem. Cycles*, 16 (4), 1078, doi:10.1029/2001GB001829,

Stott, P.A., G.S. Jones, J.A. Lowe, P. Thorne, C. Durman, T.C. Johns, J.-C. Thelen, 2006, Transient Climate Simulations with the HadGEM1 Climate Model: Causes of Past Warming and Future Climate Change. *J. Climate* **19** 2763-2782.

K.E. Taylor, 2001. Summarizing multiple aspects of model performance in a single diagram, *J. Geophys. Res.*, 106, D7, 7183-7192.

Tréguer, P., D.M. Nelson, A.J. Van Bennekom, D.J. DeMaster, A. Leynaert, and B. Quéguiner, 1995. The silica balance in the world ocean: a reestimate, *Science*, 268, 375-379

Valentini, R. (ed.) 2002. Fluxes of Carbon, Water and Energy of European Forests. Heidelberg, Springer-Verlag.

M.L. Wesely, 1989. Parameterization of surface resistances to gaseous dry deposition in regional-scale numerical models, *Atmos. Environ.*, 23, 1293-1304.

Woodward S. 2001. Modelling the atmospheric life cycle and radiative impact of mineral dust in the Hadley Centre climate model, *J. Geophys. Res.*, 106, D16, 18,155-18,166,.

Zinke, P.J., Stangenberger, A.G., Post, W.M., Emanuel, W.R. and Olson, J.S., 1986. 'Worldwide organic soil carbon and nitrogen data.' NDP-018, Carbon Dioxide Information Center, Oak Ridge National Laboratory, Oak Ridge, Tennessee, USA.